

Motifs for processes on networks

Alice C. Schwarze*

*Department of Biology, University of Washington, Seattle, WA, USA and
eScience Institute, University of Washington, Seattle, WA, USA*

Mason A. Porter†

Department of Mathematics, University of California Los Angeles, Los Angeles, CA, USA

The study of motifs in networks can help researchers uncover links between structure and function of networks in biology, the sociology, economics, and many other areas. Empirical studies of networks have identified feedback loops, feedforward loops, and several other small structures as “motifs” that occur frequently in real-world networks and may contribute by various mechanisms to important functions these systems. However, the mechanisms are unknown for many of these mechanisms. We propose to distinguish between “structure motifs” (i.e., graphlets) in networks and “process motifs” (which we define as structured sets of walks) on networks and consider process motifs as building blocks of processes on networks. Using the covariances and correlations in a multivariate Ornstein–Uhlenbeck process on a network as examples, we demonstrate that the distinction between structure motifs and process motifs makes it possible to gain quantitative insights into mechanisms that contribute to important functions of dynamical systems on networks.

I. INTRODUCTION

The study of motifs in networks has advanced the understanding of various systems in biology [1–5], economics [6, 7], social science [8, 9], and other areas. When interpreting motifs as small building blocks that can contribute to a network’s functionality, it can be important to identify motifs that are necessary, beneficial, or disadvantageous to a network’s function to help uncover the relationship between network structure and network function.

Traditionally, scientists have considered graphlets (i.e., small graphs of typically three to five nodes) as building blocks of a network’s structure and identified them as “motifs” when empirical data [1, 6, 7, 9–12] or mathematical models [13–16] indicate their importance to system function. In many studies of “real-world” networks from empirical data, researchers have compared graphlet frequencies in a network to graphlet frequencies in an appropriate random-graph null model [6, 7, 9–12]. They subsequently have concluded that graphlets that are overrepresented in the network are likely to be relevant for important functions of the system that is associated with that network. However, the results of such studies depend very sensitively on the choice of an appropriate random-graph null model [17–19], and this approach to motif identification does not uncover the mechanisms by which the identified graphlets contribute to important system functions.

Other studies have aimed to provide mechanistic insights by modeling dynamical systems on graphlets in isolation [13–16]. The design of such studies requires an *a priori* choice of a graphlet, a dynamical system or a

class of dynamical systems, and a candidate mechanism by which the graphlet facilitates an important system function. It is therefore difficult for such studies to discover new and/or unexpected mechanisms or to provide a systematic comparison of the importances of different graphlets and different mechanisms for a system function.

In the present paper, we propose a framework for connecting the study of dynamics on networks with the study of motifs in networks. We propose to distinguish between “structure motifs” (i.e., graphlets) in networks and “process motifs” (which we define in the form of structured sets of walks) on networks, and we consider process motifs as building blocks for processes on networks[20]. We demonstrate how to use process motifs to connect network structure to dynamics on networks and to dynamics-based notions of system functions. These connections lead to mechanistic and quantitative insights into the contribution of all possible structure motifs to a given system function. We give concrete examples in Section IV.

We define a *process motif* on a graph (V, E) with node set V and edge set E to be a *walk graph*, which we define to be a directed and weighted multigraph in which each edge corresponds to a walk in (V, E) and each edge’s weight corresponds to the length of the associated walk. We show examples of walk graphs in Fig. 1.

In Fig. 2, we give an overview and an example of our process-based approach to studying motifs in networks, and we indicate how our results can inform future studies of motifs in network structure. We model a system function as a real-valued function Y of the state of a dynamical system. One can identify the process motifs that are relevant for a given mathematical function Y and associate each process motif with a numerical value b that indicates its contribution to Y . From process motifs and their contributions, one can derive structure motifs that are relevant to the function Y and their contributions c to Y . Process motifs thus offer a framework for identifying

* Corresponding author: schwarze@uw.edu

† Corresponding author: mason@math.ucla.edu

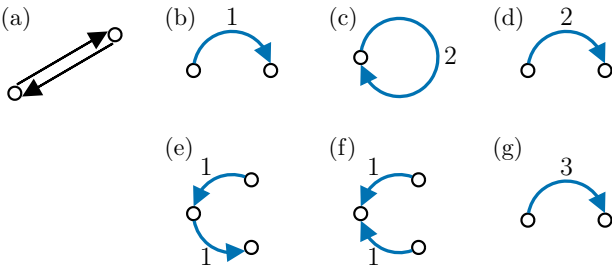


Figure 1. Examples of walk graphs. In (a), we show a small network. In (b)–(g), we show examples of associated walk graphs. The walk graphs in (b) and (c) are examples of walk graphs that use each edge in the edge set E at most once and in which each walk-graph node corresponds to a node in V . The walk graphs in (d) and (e) are examples of walk graphs in which two walk-graph nodes correspond to the same node in V . The walk graphs in (f) and (g) are examples of walk graphs that use edges in E more than once.

of functionally important graphlets (i.e., structure motifs) from mathematical models. This approach can lead detailed insights into the mechanisms by which structure motifs can affect a system function (see Section IV) [21]. One can use structure-motif contributions to rank mechanisms based on their efficiency and thereby rank structure motifs based on their importance in contributing to a system function.

As an example system, we use the multivariate Ornstein–Uhlenbeck process (mOUP), which is a popular model for noisy coupled systems [22]. It has been applied to neuronal dynamics [23], stock prices [24], the study of gene expression [25], and other systems. Properties of the mOUP are related to properties of coupled excitable systems. For example, one can derive the mOUP as a linear-response approximation of an integrate-and-fire model for excitable neurons [26, 27].

As example system properties, we examine the covariances and the correlations in the mOUP at steady state. Covariances and correlations between pairs of nodes in a network are relevant for a wide variety of research. In particular, researchers have used correlations between variables to construct networks for various applications [28–30]. For example, in networks of functional connectivity, an edge may indicate a large positive correlation between two neurons or two brain regions [28]. In networks of gene co-expression, an edge may indicate a strong correlation between the expression of two genes [29]. Additionally, existing intuitive results on simple network structures that induce covariance and correlation (see, e.g., Reichenbach’s common-cause principle [31]) make covariance and correlation interesting examples for our study. We demonstrate that our approach confirms known results about covariation between variables and that they yield additional, quantitative insights into the mechanisms by which network structure can enhance or reduce covariance or correlation between nodes.

Our process-based approach to the study of motifs on

networks yields a list of relevant process motifs (with their respective contributions to a system function) and a list of relevant structure motifs (with their respective contributions to the same system function). As we indicate in Fig. 2, these results depend both on the choice of a dynamical system and on the choice of system function. However, they do not depend on the choice of a network or a random-graph model. In Fig. 2, the arrow from the center panel to the left panel indicates how our results can inform future studies of graphlets in networks and can lead to quantitative insights into the importance of graphlets for a system function on a given network (from data or from a random-graph model) or for a random-graph model.

Our paper proceeds as follows. In Section II, we review some graph-theoretical concepts and define the notion of walk graphs, which make it possible to distinguish between structure motifs and process motifs. We also provide an overview of the use of motifs in prior studies of networks. In Section III, we show how to derive process motifs, structure motifs, and their contributions to a given property (such as a correlation) of a dynamical system. In Section IV, we give a brief introduction to the mOUP and derive process motifs and structure motifs for steady-state covariances and correlations for node pairs in the mOUP. We discuss similarities and differences between the mechanisms for covariance and correlation between nodes in the mOUP. In Section V, we conclude and discuss possible applications of our process-based approach to the study of motifs in networks. We also explain why the distinction between process motifs and structure motifs is important for many (but not all) dynamical systems on networks.

II. PROCESS MOTIFS AND STRUCTURE MOTIFS

In this section, we define process motifs and structure motifs. In Section II A, we give a brief introduction to relevant graph-theoretical concepts. In Section II B, we introduce walk graphs. We then define process motifs and structure motifs as walk graphs and connected subgraphs, respectively. To illustrate the conceptual difference between process motifs and structure motifs, we compare methods for counting walk graphs to methods for counting subgraphs in Section II C. In Section II D, we introduce the concepts of matching process motifs and matching structure motifs. (These concepts are useful for our calculations in Section IV.) In Section II E, we overview prior uses of process motifs and structure motifs in the study of networks.

A. Some graph-theoretical concepts

We now give definitions for *walks* and *trails* on networks and *paths* in networks. These words and other ter-

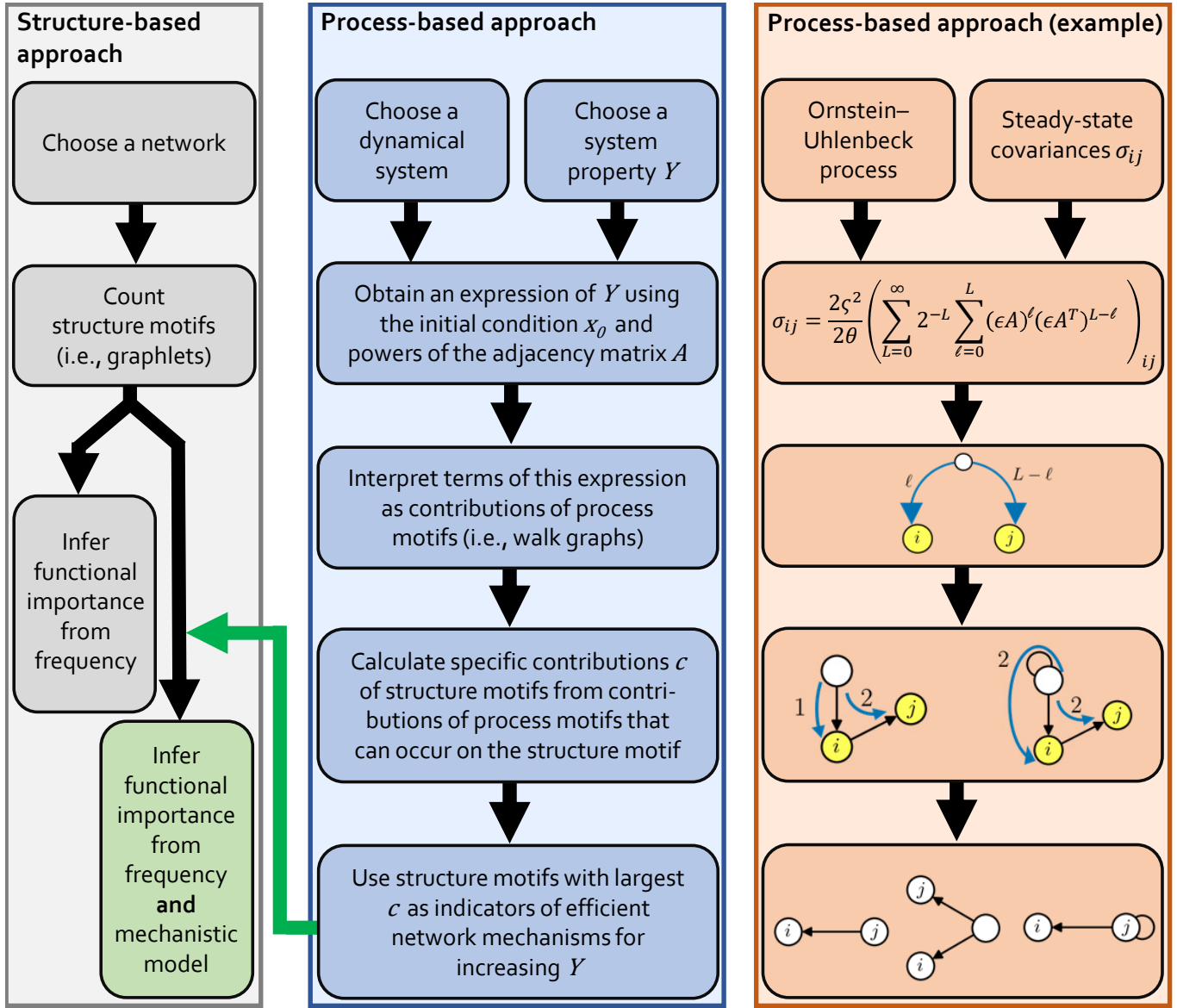


Figure 2. Comparison of a structure-based approach to the study of motifs in networks and the process-based approach that we introduce in this paper. In the right panel, we give an overview of the results of applying our approach to the study of process motifs and structure motifs that are relevant for steady-state covariances σ_{ij} (see Eq. (7)) for node pairs (i, j) in a multivariate Ornstein–Uhlenbeck process with parameters θ , ς , and ϵ and adjacency matrix \mathbf{A} (see Eq. (6)). The parameters L and ℓ characterize a process motif for σ_{ij} with walk lengths ℓ and $L - \ell$.

minology for graph-theoretical concepts are often used ambiguously, and we will need to distinguish these concepts clearly for our work in the present paper.

We consider a *network* (i.e., *graph*) to be an ordered tuple (V, E) that consists of a set V of nodes and a set $E \subseteq V \times V$ of edges [32]. If the network is *directed*, its edges $e \in E$ are ordered pairs of nodes. If the network is *undirected*, its edges $e \in E$ are unordered pairs of nodes. A *weighted* network is an ordered tuple (V, E, W) with a node set V and edge set E as before and a map W that assigns a *weight* to each edge in E . For the remainder of the present paper, we exclude W from our notation for

networks. However, our definitions and results hold for both weighted and unweighted networks, and we generally assume that edges in a network can have weights.

A *subgraph* (V', E') of a network (V, E) is a network that consists of a node set $V' \subseteq V$ and an edge set $E' \subseteq E$ [32]. A *supergraph* (V'', E'') of a network (V, E) is a network with node set $V'' \supseteq V$ and an edge set $E'' \supseteq E$ [33].

We distinguish between walks and trails on networks and paths in networks. Consider a directed or undirected

network (V, E) . A *walk* in this network is a sequence

$$w = (v_{i_1}, e_{i_1, i_2}, v_{i_2}, e_{i_2, i_3}, \dots, e_{i_{\ell-1}, i_\ell}, v_{i_\ell}, e_{i_\ell, i_{\ell+1}}, v_{i_{\ell+1}})$$

of nodes $v_{i_1}, v_{i_2}, \dots, v_{i_\ell}, v_{i_{\ell+1}} \in V$ and edges $e_{i_1, i_2}, e_{i_2, i_3}, \dots, e_{i_{\ell-1}, i_\ell}, e_{i_\ell, i_{\ell+1}} \in E$ such that each edge $e_{i,j}$ starts at node v_i and ends at node v_j [32]. The number ℓ indicates the number of edges in a walk. We call ℓ the *length* of a walk. If no edge in E appears more than once in w , the walk w is also a *trail* [32]. If no node in V and no edge in E appear more than once in w , one can use the set of nodes in w and the set of edges in w to construct a *path*. A *path* is a subgraph (V', E') that consists of a node set $V' \subseteq V$ and an edge set $E' \subseteq E$ that one can combine to construct a sequence

$$(v_{i_1}, e_{i_1, i_2}, v_{i_2}, e_{i_2, i_3}, \dots, e_{i_{\ell-1}, i_\ell}, v_{i_\ell}, e_{i_\ell, i_{\ell+1}}, v_{i_{\ell+1}})$$

of nodes and edges [32]. The number ℓ is the *length* of the path.

A *path* is a subgraph of a network. By contrast, a walk is a combination (with repetition allowed) of a network's nodes and edges [34]. One can use walks to describe many processes on networks [35–38]. Additionally, one can consider the sequence of nodes and edges in a walk to be the temporal sequence of nodes and edges that a signal, a person, or some other entity traverses.

A *closed walk* of length ℓ is a sequence

$$w = (v_{i_1}, e_{i_1 i_2}, v_{i_2}, e_{i_2 i_3}, \dots, e_{i_{\ell-1} i_\ell}, v_{i_\ell}, e_{i_\ell i_1}, v_{i_1})$$

of nodes and edges [32]. A *cycle* of length ℓ is a subgraph (V', E') that consists of a node set $V' \subseteq V$ and an edge set $E' \subseteq E$ that one can combine to construct a sequence [32]

$$(v_{i_1}, e_{i_1, i_2}, v_{i_2}, e_{i_2, i_3}, \dots, e_{i_{\ell-1}, i_\ell}, v_{i_\ell}, e_{i_\ell, i_1}).$$

One can think of a cycle as a closed path.

We say that a graph is *cyclic* if it is a cycle. It is *acyclic* if it is not a cycle and none of its subgraphs is a cycle.

An undirected network (V, E) is *connected* if for every unordered pair (i, j) of nodes in V , there exists a path from i to j . A directed network (V, E) is *strongly connected* if for every ordered pair $(i, j) \in V \times V$, there exists a path from i to j . It is *weakly connected* if its corresponding undirected network is connected.

A network has an associated *adjacency matrix* $\mathbf{A} = (a_{ij})$. If the network is unweighted, $a_{ij} \in \{0, 1\}$ and $a_{ij} = 1$ indicates an edge from node j to node i . If the network is weighted, the non-zero elements of \mathbf{A} are $a_{ij} = w(e)$, where $w(e)$ is the weight of the edge e from node j to node i .

B. Walk graphs and process motifs

Consider a directed or undirected network (V, E) . We define a *walk graph* on this network to be a weighted

and directed multigraph $(\tilde{V}, \tilde{E}, \ell)$, where \tilde{V} is a combination (with repetition allowed) of nodes in V and each edge in \tilde{E} corresponds to a walk on the associated network (V, E) . The *length* $\ell(e)$ of an edge $e \in \tilde{E}$ is the length of the corresponding walk (i.e., the number of edges that the walk on (V, E) traverses). When characterizing walk graphs, a useful property is the walk graph's *spatial length*

$$L := \sum_{e \in \tilde{E}} \ell(e).$$

A walk graph's *duration* (i.e., *temporal length*) is $T := \max_{e \in \tilde{E}} \ell(e)$. For our paper, the spatial length of walk graphs is an important quantity. For the rest of our paper, we use the term "length" for a walk graph's spatial length.

To give some examples of walk graphs, we recall the walk graphs in Fig. 1. A walk graph that consists of a single edge corresponds to a single walk on the associated network (see, e.g., Figs. 1 (b), (d), and (g)). If a walk graph consists of a single self-edge, then the walk graph corresponds to a closed walk in the associated network (see, e.g., Fig. 1 (c)).

We noted in Section II A that one can interpret a walk to describe a type of process. One can thus use a walk graph to describe a composite process that consists of several walks. We can now formally consider a *process motif* to be a small, weakly connected walk graph that affects a given function of the dynamics on a network. We consider a *structure motif* to be a small, weakly connected graph that affects a given function of the dynamics on a network.

C. Counts of process motifs and structure motifs

It is common for studies of motifs to associate motifs with a "count", "number", or "frequency" to indicate the prevalence of a given motif in a given system [10, 39, 40]. The *count* (i.e., number) of a structure motif s in a network (V, E) is the number of subgraphs of (V, E) that are isomorphic to s . We define the count of a process motif p in an unweighted network (V, E) to be the number of sets of walks in (V, E) that form a walk graph that is isomorphic to p .

For a weighted network (V, E, W) , it is useful to weight each occurrence of a process motif by the product $\pi := \prod_e w(e)$, where one takes the product of the weights of edges $e \in E$ that the walks in p traverse. (If the walks in p traverse an edge k times, the corresponding edge weight $w(e)$ appears in π with multiplicity k .) When (V, E, W) is a weighted network, we define the count of p to be the sum of edge-weight products π for each walk graph on (V, E, W) that is isomorphic to p .

The counts of structure motifs in a network and the counts of process motifs are related to each other. Each structure motif s has an associated set P_s of process motifs that can occur on it. Consequently, a change in the

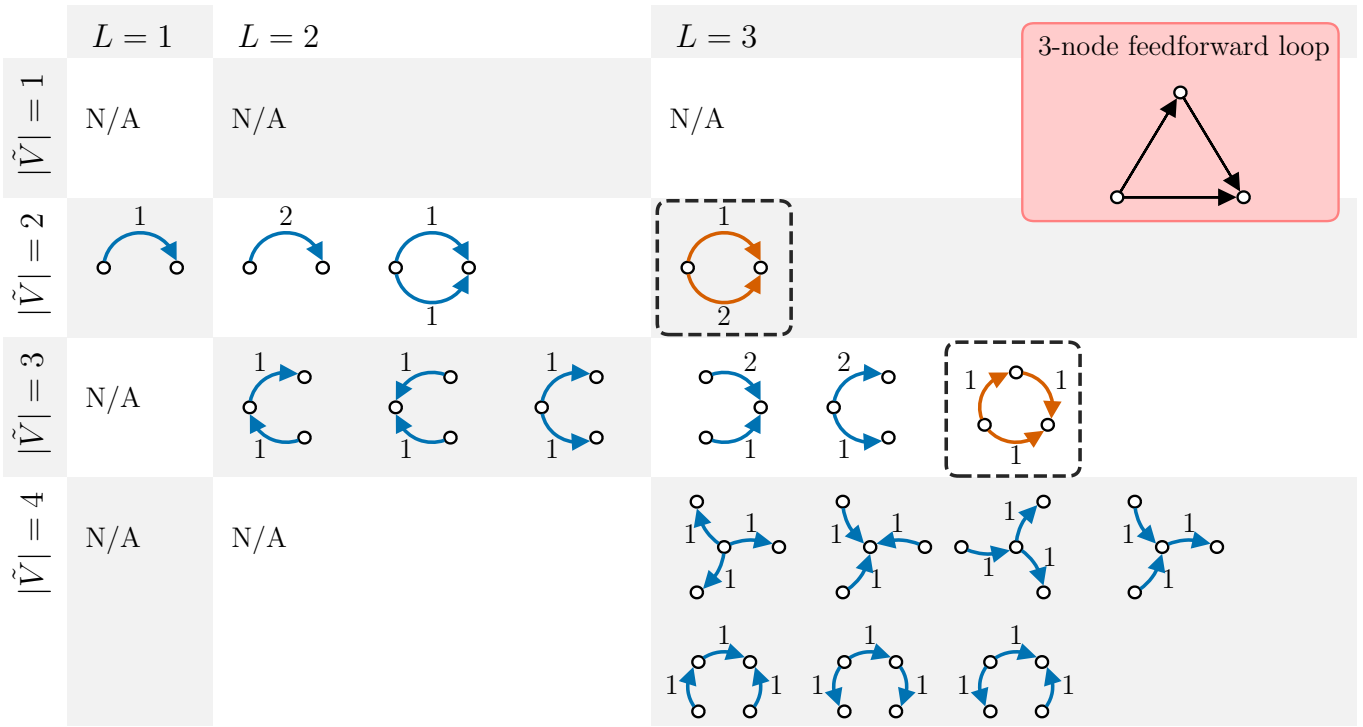


Figure 3. Walk graphs that can occur on a 3-node feedforward loop. We sort walk graphs according to their length L and their number $|\tilde{V}|$ of nodes. The numerical edge labels on walk graphs indicate the length of an edge. Some walk graphs occur on the 3-node feedforward loop but not on the 3-node feedback loop. We use orange edges and boxes with dashed boundaries to distinguish these walk graphs from others. The pink inset in the top-right corner shows the structure of a 3-node feedforward loop.

number of motifs of type s (i.e., the count of s) leads to a change in the counts for each $p \in P_s$. To illustrate this relationship between counts of structure motifs and counts of process motifs, we consider two small example networks: a 3-node feedforward loop and a 3-node feedback loop [10]. In Fig. 3, we show all length- L walk graphs that can occur on a 3-node feedforward loop for $L \leq 3$. In Fig. 4, we show all length- L walk graphs that can occur on a 3-node feedback loop for $L \leq 3$.

From comparing Figs. 3 and 4, we observe that some walk graphs can occur on the 3-node feedforward loop but not on the 3-node feedback loop, and vice versa. The differences between the walk graphs for the 3-node feedforward loop and the walk graphs for the 3-node feedback loop illustrate that the structure of a network constrains the structures of walk graphs that can occur on it. The 3-node feedforward loop is an acyclic network with a maximum trail length of 2. Because the feedforward loop is a directed acyclic graph (DAG), its associated walk graphs are also acyclic. Walk graphs on a DAG with a maximum trail length of 2 cannot have edges of length $\ell(e) > 2$.

The structure of the 3-node feedback loop leads to other constraints on the structures of associated walk graphs. For example, a walk graph that can occur on the 3-node feedforward loop but not on the 3-node feedback loop is the circular walk graph with $|\tilde{V}| = 2$ and $L = 3$ in Fig. 3. This walk graph consists of a length-1

edge and a length-2 edge that share both their starting node and their ending node.

D. Matching process motifs and matching structure motifs

Consider the set P_s of process motifs that can occur on a structure motif s and the set S_p of structure motifs on which a process motifs p can occur. If one does not specify a number $|\tilde{V}|$ of nodes and a length L for a process motif, the set P_s for any s with one or more edges includes infinitely many process motifs because a process motif can use each edge of the structure motif infinitely many times. Conversely, for a given process motif p , the set S_p includes infinitely many structure motifs because one can add nodes or edges to any $s \in S_p$ to obtain another element of S_p .

Most elements in P_s are very long process motifs, and most elements of S_p are very large structure motifs. Traditionally, studies of motifs on networks have focused on small motifs: process motifs with length $L \leq 4$ [41–43] and structure motifs with up to five nodes [10, 39]. To associate small process motifs with small structure motifs and vice versa, we define *matching process motifs* and *matching structure motifs*. For a given process motif p , a matching structure motif s_p^* is a structure motif on

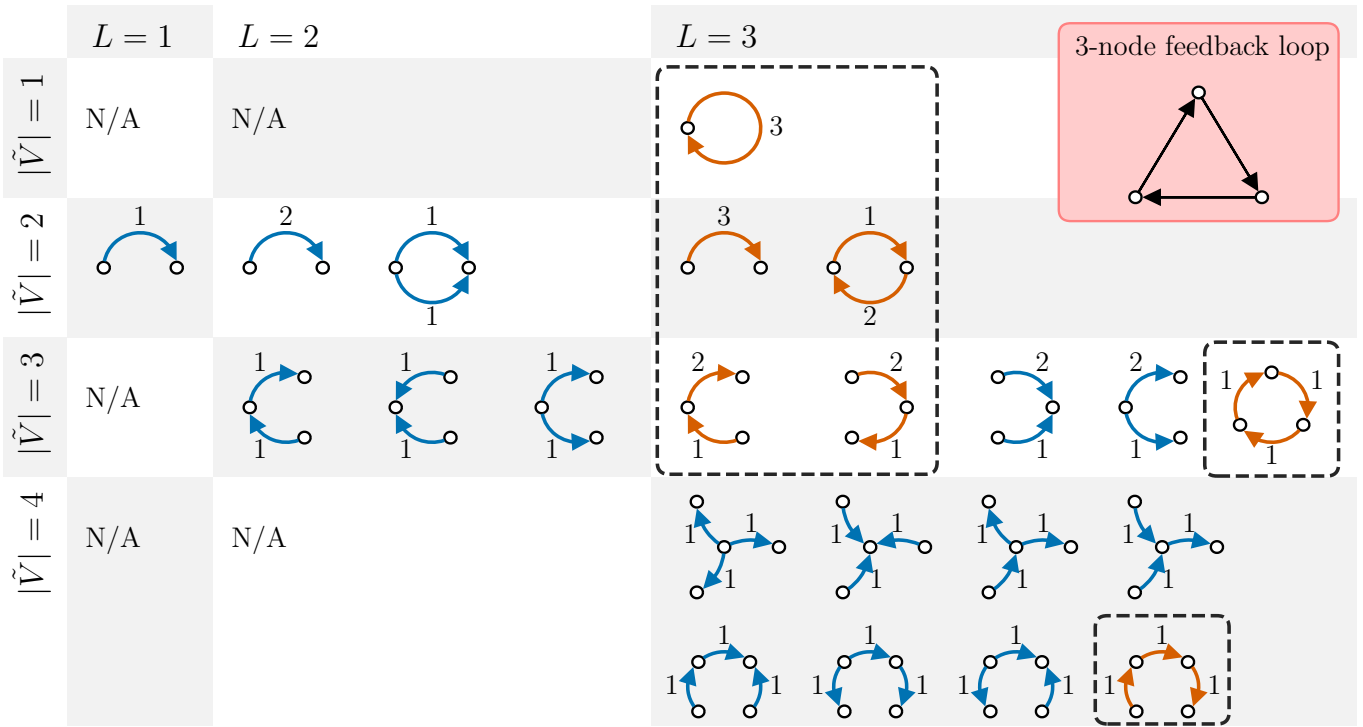


Figure 4. Walk graphs that can occur on a 3-node feedback loop. Some walk graphs occur on the 3-node feedforward loop but not on the 3-node feedback loop. We use orange edges and boxes with dashed boundaries to distinguish these walk graphs from others. The inset in the top-right corner shows the structure of a 3-node feedback loop.

which p can occur while using each edge in s_p^* exactly once. Conversely, for a given structure motif s , a *matching process motif* is a process motif that can occur on s while using each edge in s exactly once.

For a structure motif s with a finite number of edges, the set P_s^* of matching process motifs has a finite number of elements. For a process motif p with a finite length L , the set S_p^* of matching structure motifs also has a finite number of elements.

In Fig. 5, we show sets of matching process motifs and sets of matching structure motifs for several structure motifs and process motifs, respectively. Structure motifs that do not include cycles have only acyclic matching process motifs. Therefore, for a given number of edges, structure motifs that include cycles (e.g., the structure motifs in the second and fourth row in the left table of Fig. 5) have more matching process motifs than acyclic structure motifs (e.g., the structure motifs in the first and third row in the left table of Fig. 5). Accordingly, acyclic process motifs have more matching structure motifs than cyclic process motifs.

In general, a structure motif can have many matching process motifs and a process motif can have many matching structure motifs. Motif-based research that aims to link network structure to dynamics on networks requires careful consideration of these matching motifs. In Section IV, we demonstrate the importance of these considerations using steady-state covariance and steady-state

correlation of a multivariate Ornstein–Uhlenbeck process (mOUP) as an example.

E. Previous work on process motifs and structure motifs

To the best of our knowledge, previous research on network motifs has not distinguished explicitly between process motifs and structure motifs. Instead, studies have been concerned either with process motifs or with structure motifs, and they have referred to either as “network motifs”. In this section, we give an overview of research on “network motifs” and explain which of the reviewed studies concern process motifs and which concern structure motifs.

Many reviews of network motifs have credited Milo et al. [10] for the idea of characterizing networks by connected subgraphs that are more frequent in a network than one would expect [2, 44, 45]. (The expectation is usually based on the frequency of connected subgraphs in a configuration model [3, 10, 19].) Other researchers have indicated that the search for frequent patterns in networks was already a topic of interest in, for example, ecology in the 1970s [3].

Milo et al. [10] compared several gene-regulatory networks, a neural network for the worm *C. elegans*, several food webs, several electronic circuits, and the World

Structure motif	Matching process motifs		Process motif	Matching structure motifs	
					
					
					
					

Figure 5. Matching sets of structure motifs and matching sets of process motifs. On the left, we show four structure motifs and their sets of matching process motifs. On the right, we show four process motifs and their sets of matching structure motifs.

Wide Web. They viewed gene-regulatory networks and neural networks as systems “that perform information processing” and reported that these networks have similar overrepresented connected subgraphs. They also reported that other networks, such as food webs and the World Wide Web, did not have similar overrepresented subgraphs as the considered gene-regulatory networks and the *C. elegans* neural network. Subsequently, many researchers have studied various networks by identifying overrepresented connected subgraphs (e.g., see [6, 7, 9, 11, 12]). In the corresponding publications, researchers used “motif” or “network motif” to refer to an overrepresented connected subgraph, which are structure motifs.

Closely related to the idea of characterizing networks by examining overrepresented subgraphs is the idea of characterizing networks based on the numbers or frequencies of one or several specified subgraphs [46–58]. For example, several researchers have used the number of triangles in an undirected network’s structure to characterize networks [46, 47] or to explain aspects of dynamics on these networks [48, 49]. Others have used the numbers of different structure motifs with 3 or 4 nodes to compare networks [50–55] or to explain aspects of dynamics on them [56–58]. In some of these studies, researchers have considered “network motifs” to be small connected subgraphs without the requirement of overrepresentation with respect to a null model [48, 55]. The “network motifs” in these studies are also structure motifs.

Estrada and Rodríguez-Velázquez [59] proposed a measure of centrality that exploits the relationship between structure motifs and process motifs in a network. Their centrality measure, called “subgraph centrality”, is a weighted sum of closed walks that start and end at a node. Noting that “each closed walk is associated

with a connected subgraph” [59], Estrada and Rodríguez-Velázquez concluded that one can use a weighted sum of closed walks that start and end at a node as a measure of the count of cyclic graphlets that include that node. Their rationale for proposing subgraph centrality thus makes implicit use of the fact that each process motif that consists of a single closed walk has a corresponding matching structure motif that is a cycle.

In several theoretical studies of dynamical systems on networks, researchers have used process motifs when interpreting the results of their derivations [23, 27, 41–43, 60, 61]. In theoretical neuroscience, a common approach to connect network structure with system functions is to linearize nonlinear dynamical systems about an equilibrium point and consider the effect of small perturbations on the dynamics. When deriving an approximation to the system state or a function of the system state for perturbations with a small prefactor ϵ , one can sometimes associate the terms of the approximation with process motifs. Researchers have used this approach to find process motifs for “neural complexity” [23, 41, 62], information content [42], transfer entropy [43], cross-correlations [60], and other properties of stochastic dynamical systems on networks [27, 61]. In these studies, the order of ϵ in the approximation indicates the length or duration of the corresponding process motif.

Barnett et al. [23, 41] considered the mOUP on a network and derived an approximation for neural complexity up to third order in ϵ . They associated the terms of their approximation with “graph motifs” with up to 3 edges [41]. These graph motifs are process motifs of length $\ell \leq 3$. Lizier et al. [42] derived an approximation for the information content of a multivariate Gaussian autoregressive process on a network up to fourth order in ϵ and associated terms of the approximation with process

motifs with up to four edges. For the same dynamical system, Novelli et al. [43] recently derived process motifs for pairwise transfer entropy up to fourth order in ϵ . Trousdale et al. [60] derived an approximation for cross-correlations of a system of coupled integrate-and-fire neurons [63] to arbitrary order in ϵ . They associated each order of their approximation with a “submotif” that included time-ordered edges. These submotifs are unions of process motifs. Hu et al. [27] approximated a measure of “global coherence” for the mOUP on a network to arbitrary order in ϵ . They associated each order of their approximation with a normalized count (which they called a “motif cumulant”) of a so-called “ (n, m) motif”. The “ (n, m) motifs” are equivalent to the process motifs that we derive for covariances of the mOUP in Section IV. Jovanovic and Rotter [61] derived approximations for covariance and the third joint cumulant, which is a measure of dependence between three variables, for a network of coupled Hawkes processes. They associated their approximation for covariance with 2-edge process motifs and their approximation of the third joint cumulant with process motifs with three or more edges.

Other applications of dynamics on networks that are relevant to the perspective of this paper include the spread of opinions [64] and the spread of infectious diseases [65]. In probabilistic compartment models on networks, which are the most common type of model for studying infectious diseases on networks, the probability that a node is infected can depend on the infection probability of other nodes [66]. For a subset of the nodes, it is common to approximate joint moments of infection probabilities by products of moments (if there is only a single node in the subset) or joint moments (if there are two or more nodes in the subset) of the node(s) [66, 67]. In doing so, one selects the joint moments of node-infection probabilities on some motifs — typically, connected pairs or connected triples of nodes — to be relevant for a spreading process and other joint moments to be negligible [68, 69]. The motifs in these models can be process motifs or structure motifs. Researchers have used DAGs to describe the spread of behavior, norms, and ideas [70] and the spread of infectious diseases [71, 72] on networks. One can view subgraphs of these so-called “dissemination trees” [70] and “epidemic trees” [71, 72] as process motifs.

For many studies of the spread of infectious diseases, either the choice of compartment model (e.g., susceptible–infected–recovered [73, 74]) or the choice of network structure (e.g., if it is locally tree-like [75, 76]) constrains the number of relevant process motifs such that, for structure motif with five or fewer edges, there is only one relevant process motif that can occur on it. Because of this one-to-one correspondence between process motifs and structure motifs, the distinction between them is irrelevant for these models of disease spread, provided that one considers only small motifs (of five edges or fewer). In Section V C, we discuss when the distinction between process motifs and structure motifs is relevant and when it is not.

III. USING PROCESS AND STRUCTURE MOTIFS TO STUDY FUNCTIONS OF DYNAMICS ON NETWORKS

In this section, we motivate the use of process motifs for the study of dynamical systems on networks. We formally define contributions of process motifs and structure motifs to real-valued functions of the state of a dynamical system on a network. We focus on linear dynamical systems. In general, one cannot use the same approach to directly study nonlinear dynamical systems, although one can apply our approach to linearizations of nonlinear dynamical systems.

A. Linking process motifs to properties of dynamics on networks

Consider a linear dynamical system

$$\frac{d\mathbf{x}_t}{dt} = \mathbf{F}(\mathbf{A})\mathbf{x}_t, \quad (1)$$

where \mathbf{x}_t is a column vector that describes the current system state, the system has the initial state $\mathbf{x}_0 = \mathbf{x}_{t=0}$, and \mathbf{F} is a matrix-valued function of the adjacency matrix \mathbf{A} of a network. Observables of the linear dynamical system in Eq. (1) are functions of \mathbf{x}_t and \mathbf{F} , and they are thus functions of \mathbf{A} and \mathbf{x}_0 . (For systems at steady state or a system with uniformly distributed initial values $x_{01} = x_{02} = x_{03} = \dots$, one can often remove the dependence on \mathbf{x}_0 and describe functions of the dynamical system as functions of only \mathbf{A} .) One can thus view a function of the linear dynamical system (1) as a superposition of walks or a superposition of walk graphs on a network.

This view motivates the approach that we take in the present paper. We study how a function of a linear dynamical system emerges via the superposition of process motifs, which are structured sets of walks in an associated network. After identifying relevant process motifs for a given property of a dynamical system on a network, one can establish links between dynamics on networks and network structure by identifying the structure motifs on which the relevant process motifs can occur. This approach results in a set of structure motifs that contribute to the desired system function along with explanations of the mechanisms by which these structure motifs contribute to this function. When it is possible to quantify the contribution of process motifs to the function of interest, one can also quantify the contribution of structure motifs. In Section IV, we demonstrate our approach using the covariances and the correlations in the mOUP at steady state as examples. In the remainder of Section III, we explain how we formalize links between process motifs and structure motifs.

B. Contributions of process motifs and structure motifs

Consider a scalar property $Y = f(\mathbf{A})$ of a linear dynamical system on a network with adjacency matrix \mathbf{A} . Assume that we have identified the relevant process motifs p_1, p_2, \dots, p_k and their real-valued contributions $b_{p_1}, b_{p_2}, \dots, b_{p_k}$ to Y , so that, in a network on which p_i has the count n_{p_i} , we can compute Y from

$$Y = \sum_{i=1}^k b_{p_i} n_{p_i}, \quad (2)$$

which is a weighted sum of counts of process motifs.

There are several ways that one can define a structure motif's contribution to Y . For example, one can define the contribution c of a structure motif s to be the real-valued sum of all contributions b_p of all process motifs p that can occur on s . This association is intuitive and tends to be computationally easy to obtain. For a linear dynamical system, one can compute c directly from $c = f(\mathbf{A}')$, where \mathbf{A}' is the adjacency matrix of the structure motif s . We call c the *total contribution* of a structure motif s to Y .

There are some disadvantages of using c to characterize a structure motif's contribution to Y . For example, there is no straightforward way of expressing Y as a weighted sum of counts of structure motifs. Moreover, if all $b_{p_i} > 0$, large structure motifs tend to contribute much more to Y than small structure motifs, because large structure motifs have much larger sets of process motifs that can occur on them than small structure motifs.

To address these two issues, we propose a different definition for the contribution of a structure motif to Y . The contribution \hat{c} of a structure motif s is the sum of contributions b_p of process motifs p that can occur on s but not on any subgraph of s . We call \hat{c} the *specific contribution* of a structure motif. One can express Y as the sum

$$Y = \sum_i \hat{c}_{s_i} n_{s_i} \quad (3)$$

of weighted counts n_{s_i} of structure motifs s_i . A contribution \hat{c}_s of a structure motif s is not necessarily larger than the contribution \hat{c}_t of a subgraph t of s . As we demonstrate in Section IV, the specific contribution \hat{c}_s tends to be smaller than the specific contributions \hat{c}_t of subgraphs. A drawback of using \hat{c} to characterize the contribution of structure motifs to Y is that specific contributions are much harder to compute than total contributions. In general, the computation of a specific contribution \hat{c}_s requires the computation of \hat{c}_t for all subgraphs t of s . One can compute the specific contribution of a structure motif s recursively via

$$\hat{c}_s = c_s - \sum_{t \subset s} \hat{c}_t, \quad (4)$$

where we use $t \subset s$ to denote that t is a proper subgraph of s . Alternatively, one can use the mean total contributions $\langle c \rangle_{m'}$ of subgraphs of s with m' edges to compute \hat{c}_s . That is,

$$\hat{c}_s = \sum_{m'=1}^m \left\{ \left[\binom{m}{m'} \sum_{\mathbf{q} \in \mathcal{Q}(m-m')} (-1)^{|\mathbf{q}|} \mathbf{q}! \right] \langle c \rangle_{m'} \right\}, \quad (5)$$

where m is the number of edges in s , the set $\mathcal{Q}(m-m')$ is the set of integer compositions [77] of $m-m'$, and the sequence $\mathbf{q} = (q_1, q_2, \dots, q_k)$ is an integer composition of $m-m'$ with k elements. In Eq. (5), we denote the number of elements in a sequence \mathbf{q} by $|\mathbf{q}|$ and the multinomial coefficient of a sequence \mathbf{q} of integers by “ $\mathbf{q}!$ ”. We derive Eq. (5) in Appendix A. For structure motifs with $m > 2$ edges, it is computationally easier to calculate \hat{c} from Eq. (5) than from Eq. (4).

IV. COVARIANCE AND CORRELATION FOR THE MULTIVARIATE ORNSTEIN–UHLENBECK PROCESS

In this section, we demonstrate our process-based approach for studying motifs in networks. As an example, we examine steady-state covariances and steady-state correlations in the mOUP. We derive contributions of process motifs and total and specific contributions of structure motifs to covariances and correlations in the mOUP at steady state. We then discuss the relationship between specific contributions of structure motifs and network mechanisms that contribute to steady-state covariances and steady-state correlations in the mOUP.

A. The Ornstein–Uhlenbeck process

Uhlenbeck and Ornstein [78] proposed a stochastic process to describe Brownian motion under the influence of friction. Among the many extensions of their model, the mOUP is a popular model for coupled noisy systems, including neuronal dynamics [23], stock prices [24], and gene expression [25]. In these studies, the mOUP with n variables describes the dynamics on a network with n nodes, where the state of each node represents a neuron, stock, or gene-expression level.

One can describe the mOUP via

$$d\mathbf{x}_{t+dt} = \theta(\epsilon\mathbf{A} - \mathbf{I})\mathbf{x}_t dt + \varsigma dW_t, \quad (6)$$

where we use a column vector $\mathbf{x}_t \in \mathbb{R}^N$ to describe the state of the process. The process has an adjacency matrix \mathbf{A} , which can be directed and/or weighted, and a multivariate Wiener process W_t . The *reversion rate* $\theta > 0$, the *noise amplitude* ς^2 , and the *coupling parameter* $\epsilon > 0$ are parameters of the mOUP.

We consider a signal to be a (temporary) deviation of a node's state from its mean. The coupling parameter

sets the rate at which a signal's amplitude increases or decreases when it is transmitted from one node to another. The parameter θ is the rate at which a signal's amplitude increases or decreases over time. It thus determines the expected speed at which a node's state reverts to its mean. Because of this connection between θ and the speed of signal decay in the mOUP, many researchers refer to θ as the *reversion rate* [79–81].

If all eigenvalues of $\epsilon\mathbf{A} - \mathbf{I}$ have negative real parts, the mOUP has a single stationary distribution. We then say that the mOUP is a process with *signal decay* because, in this process, a signal's amplitude decreases with time. Denoting the spectral radius of a matrix by $\rho(\cdot)$, a sufficient condition for signal decay is $\rho(\epsilon\mathbf{A}) < 1$.

The mOUP with signal decay is a Markov process. Its stationary distribution is a multivariate normal distribution $\mathcal{N}(0, \Sigma)$ centered at $\langle \mathbf{x} \rangle = 0$ with covariance matrix $\Sigma := \langle \mathbf{x}_t \mathbf{x}_t^T \rangle$ [23]. The mOUP with signal decay has the steady-state covariance matrix

$$\Sigma = \frac{\varsigma^2}{2\theta} \sum_{L=0}^{\infty} \sum_{\ell=0}^{\infty} 2^{-L} \binom{L}{\ell} (\epsilon\mathbf{A})^\ell (\epsilon\mathbf{A}^T)^{L-\ell}. \quad (7)$$

Barnett et al. [41] derived Eq. (7) for the mOUP with $\theta = \varsigma = 1$. In Appendix B, we show that Eq. (7) also holds for arbitrary choices of $\theta > 0$ and $\varsigma > 0$.

In the remainder of this section, we derive and compare process motifs and structure motifs for covariance, variance, and correlation for the mOUP at steady state.

B. Process motifs for covariance and correlation

We now derive process motifs and process-motif contributions for steady-state covariances and steady-state correlations in the mOUP.

1. Process motifs for covariance

We introduce the shorthand notation

$$b_{L,\ell} := 2^{-(L+1)} \binom{L}{\ell} \frac{\varsigma^2}{\theta}$$

and $\mathbf{N}_{L,\ell} := (\epsilon\mathbf{A})^\ell (\epsilon\mathbf{A}^T)^{(L-\ell)}$ to write

$$\Sigma = \sum_{L=0}^{\infty} \sum_{\ell=0}^L \epsilon^L b_{L,\ell} \mathbf{N}_{L,\ell}. \quad (8)$$

The (i, j) -th element of $\mathbf{N}_{L,\ell}$ corresponds to a count n_p of process motifs p for the covariance between nodes i and j . The matrix $\mathbf{N}_{L,\ell}$ is not necessarily symmetric. However, the (i, j) -th element of $\mathbf{N}_{L,\ell}$ is equal to the (i, j) -th element of $\mathbf{N}_{L,L-\ell}$.

Equation (8) indicates that one can compute the covariances of the mOUP as a weighted sum of counts of process motifs. A process motif that contributes to the

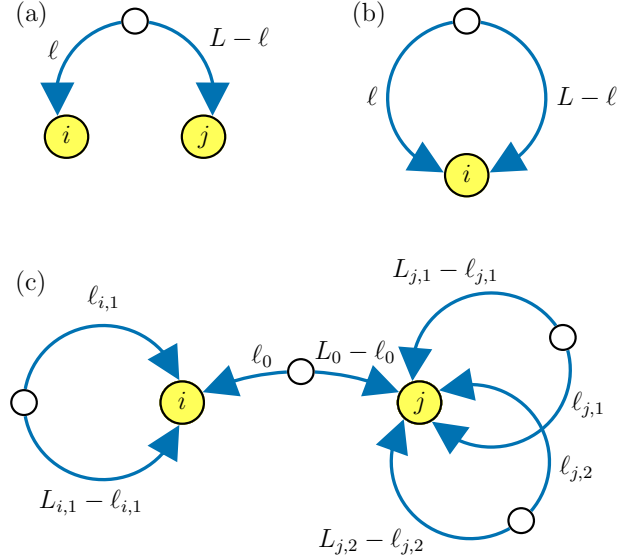


Figure 6. Process motifs for (a) covariance, (b) variance, and (c) correlation.

covariance between nodes i and j is a walk graph with three nodes and two edges. Two of the walk-graph nodes correspond to nodes i and j in the network. We call these walk-graph nodes the *focal nodes* of this process motif. All process motifs for covariance also include a third walk-graph node, which we call the “source node” and which can correspond to any node in a network. Each edge in this process motif corresponds to a walk from the source node to one of the two focal nodes. We show a diagram of a process motif that contributes to covariance in Fig. 6(a). One can characterize a process motif of this form by the two parameters $L \in \{0, 1, 2, \dots\}$ and $\ell \in \{0, \dots, L\}$. The parameter L is the length of a process motif; the parameter ℓ is the length of the walk from the source node to node i . The contribution of each process motif to the covariance is $b_{L,\ell}$.

The process motifs for covariance are consistent with properties of covariation in a system of coupled random variables. A covariance σ_{ij} measures the joint “variability” of two random variables x_i and x_j [82], where one takes variability to indicate a variable's deviation from its mean. This joint variability of x_i and x_j can arise from several causes [31]:

1. Variability in x_i induces variability in x_j if there is a path from node i to node j .
2. Variability in x_j induces variability in x_i if there is a path from node j to node i .
3. Variability in a third variable x_k induces variability in both x_i and x_j if there are paths from k to i and from k to j .

We now compare the contributions of different process

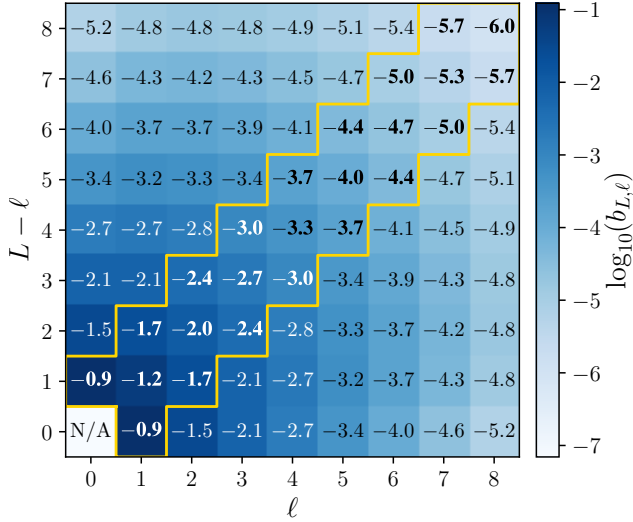


Figure 7. Contributions $b_{L,\ell}$ of process motifs for covariance with parameters (L, ℓ) for $\theta = 1$, $\varsigma = 1$, and $\epsilon = 0.49$. The length L increases along the diagonal from the bottom left to the top right. We indicate the parameter pairs for the largest contributions for each value of L by bold labels and delineate them with yellow line segments.

motifs to covariance. In Fig. 7, we show the contributions $b_{L,\ell}$ of process motifs to covariance. The length L increases along the diagonal from the bottom left to the top right. We indicate the parameter pairs with the largest contribution for each value of L by bold labels and delineate them with yellow line segments. For even L , contributions are maximal when $\ell = L/2$. For odd L , contributions are maximal when $\ell = (L \pm 1)/2$. Comparing the contributions of process motifs of different lengths, we find that short process motifs (bottom left) tend to contribute more to covariances than long process motifs. These results are consistent with the notion that covariances and correlations should decay with the distance that a signal travels [83]. The result that a process motif with $\ell = L/2$ contributes more to covariance than any other process motif with the same length L is consistent with the notion that a signal that reaches two nodes i and j at the same time contributes more to the covariance or correlation between i and j than signals that reach i and j at different times.

2. Process motifs for variance

A diagonal element of Σ indicates the variance of a node in the mOUP. By merging the focal nodes in Fig. 6(a), one obtains the process motifs that contribute to the variance of a node i (see Fig. 6(b)). Such a process motif includes two nodes and two edges. It includes a source node and a single focal node i . Its two edges correspond to two walks from the source node to node i .

We write

$$\Sigma = \frac{\varsigma^2}{2\theta} \mathbf{I} + \Sigma^{(1+)}, \quad (9)$$

where

$$\Sigma^{(1+)} := \sum_{L=1}^{\infty} \sum_{\ell=0}^L \epsilon^L b_{L,\ell} \mathbf{N}_{L,\ell}, \quad (10)$$

to separate the variance contribution $\frac{\varsigma^2}{2\theta} \mathbf{I}$ (which is independent of a network's structure) from structure-dependent variance contributions $\Sigma^{(1+)}$ (which includes all terms of Eq. (8) that are $O(\epsilon^k)$, with $k \geq 1$). We interpret the two terms in Eq. (9) as indicators of two mechanisms by which variance arises in the mOUP:

1. Gaussian white noise in each node induces the 0-th order contribution to variance. This effect contributes a value of $\varsigma^2/(2\theta)$ to the variance of the state variable x_i at each node i . This contribution is determined by the noise strength ς and the mean reversion rate θ . It is independent of a network's structure.
2. The variance of a state variable x_i exceeds its noise-induced base value of $\varsigma^2/(2\theta)$ when it receives input from other nodes via in-edges or from itself via a self-edge. For a node i , these network-dependent contributions are large when there are many process motifs for variance that have node i as their focal node. This is the case when node i is part of many cycles in a network or when many redundant paths or trails in a network connect other nodes to node i . Intuitively, cycles can reinforce variance of a node i . Redundant paths or trails that lead to node i can amplify input that i receives from other nodes.

3. Process motifs for correlation

One obtains the elements r_{ij} of the correlation matrix \mathbf{R} via

$$r_{ij} := \sigma_{ij} / \sqrt{\sigma_{ii}\sigma_{jj}}. \quad (11)$$

To replace the square root in the denominator of Eq. (11), we use the Taylor-series expansion

$$\frac{1}{\sqrt{x}} = \sum_{k=0}^{\infty} \frac{(-1)^k}{2 \cdot 4^k} \binom{2k}{k} x_0^{-\frac{2k+1}{2}} (x - x_0)^k, \quad (12)$$

which we obtain from expanding about the point $x_0 > 0$. The radius of convergence of the expansion (11) is equal to x_0 . We set $x_0 = \varsigma^2/(2\theta)$ and substitute Eq. (12) for $1/\sqrt{\sigma_{ii}}$ and $1/\sqrt{\sigma_{jj}}$ to obtain

$$\begin{aligned}
r_{ij} &= \frac{2\theta}{\zeta^2} \sigma_{ij} \sum_{k_1=0}^{\infty} \sum_{k_2=0}^{\infty} \left(-\frac{\theta}{2\zeta^2} \right)^{k_1+k_2} \binom{2k_1}{k_1} \binom{2k_2}{k_2} \left(\sigma_{ii} - \frac{\zeta^2}{2\theta} \right)^{k_1} \left(\sigma_{jj} - \frac{\zeta^2}{2\theta} \right)^{k_2} \\
&= \frac{2\theta}{\zeta^2} \sigma_{ij} \sum_{k_1=0}^{\infty} \sum_{k_2=0}^{\infty} \left(-\frac{\theta}{2\zeta^2} \right)^{k_1+k_2} \binom{2k_1}{k_1} \binom{2k_2}{k_2} \left(\sigma_{ii}^{(1+)} \right)^{k_1} \left(\sigma_{jj}^{(1+)} \right)^{k_2},
\end{aligned} \tag{13}$$

where $\sigma_{ii}^{(1+)}$ and $\sigma_{jj}^{(1+)}$ are elements of $\Sigma^{(1+)}$ (see Eq. (10)). Equation (13) is a valid expression for r_{ij} whenever the sums in Eq. (13) converge. Whenever Eq. (13) converges, we say that the mOUP has *short-range* signal decay. We derive a sufficient condition for short-range signal decay in Appendix C.

From Eq. (10), we see that one can express $\sigma_{ii}^{(1+)}$ as a sum over the two indices L and ℓ . Consequently, one can express the k -th power of $\sigma_{ii}^{(1+)}$ as a sum over the $2k$ indices $L_1, \ell_1, L_2, \ell_2, \dots, L_k, \ell_k$. We use the multisets

$$\begin{aligned}
\phi_i &:= \{(L_{i,1}, \ell_{i,1}), (L_{i,2}, \ell_{i,2}), \dots, (L_{i,k_1}, \ell_{i,k_1})\}, \\
\phi_j &:= \{(L_{j,1}, \ell_{j,1}), (L_{j,2}, \ell_{j,2}), \dots, (L_{j,k_2}, \ell_{j,k_2})\}
\end{aligned}$$

of pairs of indices to write

$$r_{ij} = \frac{2\theta}{\zeta^2} \sigma_{ij} \sum_{\phi_i, \phi_j} \left\{ \left(-\frac{\theta}{2\zeta^2} \right)^{|\phi_i|+|\phi_j|} \binom{2|\phi_i|}{|\phi_i|} \binom{2|\phi_j|}{|\phi_j|} \left[\prod_{k'=1}^{|\phi_i|} b_{L_{i,k'}, \ell_{i,k'}} (\mathbf{N}_{L_{i,k'}, \ell_{i,k'}})_{ii} \right] \left[\prod_{k'=1}^{|\phi_j|} b_{L_{j,k'}, \ell_{j,k'}} (\mathbf{N}_{L_{j,k'}, \ell_{j,k'}})_{jj} \right] \right\},$$

where $|\phi_i|$ denotes the number of pairs in ϕ_i . We use \sum_{ϕ_i, ϕ_j} to denote the double summation over all possible multisets of pairs (L, ℓ) of non-negative integers with $\ell \leq L$. We can thus express correlation as a weighted sum of counts of process motifs:

$$r_{ij} = \sum_{L_0, \ell_0, \phi_i, \phi_j} b_{L_0, \ell_0, \phi_i, \phi_j} \mathbf{N}_{L_0, \ell_0, \phi_i, \phi_j},$$

where

$$b_{L_0, \ell_0, \phi_i, \phi_j} := \frac{2\theta}{\zeta^2} \sum_{\phi_i, \phi_j} \left(-\frac{\theta}{2\zeta^2} \right)^{|\phi_i|+|\phi_j|} \binom{2|\phi_i|}{|\phi_i|} \binom{2|\phi_j|}{|\phi_j|} b_{L_0, \ell_0} \prod_{(L, \ell) \in \phi_i} b_{L, \ell} \prod_{(L, \ell) \in \phi_j} b_{L, \ell}$$

and

$$\mathbf{N}_{L_0, \ell_0, \phi_i, \phi_j} := (\mathbf{N}_{L_0, \ell_0})_{ij} \prod_{(L, \ell) \in \phi_i} (\mathbf{N}_{L, \ell})_{jj} \prod_{(L, \ell) \in \phi_j} (\mathbf{N}_{L, \ell})_{jj}.$$

The parameters L_0 and ℓ_0 and the parameter sets ϕ_i and ϕ_j characterize a process motif for correlation. A process motif for correlation consists of a process motif for covariance with focal nodes i and j , a number $|\phi_i| \geq 0$ of process motifs for variance with positive length and focal node i , and a number $|\phi_j| \geq 0$ of process motifs for variance with positive length and focal node j . We show a diagram of a process motif that contributes to correlation in Fig. 6(c). Both $|\phi_i|$ and $|\phi_j|$ can be equal to 0, so process motifs for covariance are also process motifs for correlation.

A contribution $b_{L_0, \ell_0, \phi_i, \phi_j}$ has a real non-zero value. All process motifs for correlation affect correlations, but not all process motifs for correlation contribute positively to correlations. The magnitude of $b_{L_0, \ell_0, \phi_i, \phi_j}$ is propor-

tional to the contributions $b_{L, \ell}$ of the included process motifs for variance and covariance. One can construct process motifs for correlation with large contributions $b_{L_0, \ell_0, \phi_i, \phi_j}$ from process motifs for variance and covariance with large contributions to $b_{L, \ell}$.

To illustrate the effect of the number of included variance process motifs on the contribution of a process motifs to correlation, we show contributions of different process motifs to correlation in Fig. 8. We observe that the sign of $b_{L_0, \ell_0, \phi_i, \phi_j}$ is positive when the overall number of included process motifs for variance is even and is negative otherwise. The magnitude of $b_{L_0, \ell_0, \phi_i, \phi_j}$ decreases as one adds more process motifs for variance at either of the two focal nodes (i and j). For a given process-motif length, the process motifs that contribute most to corre-

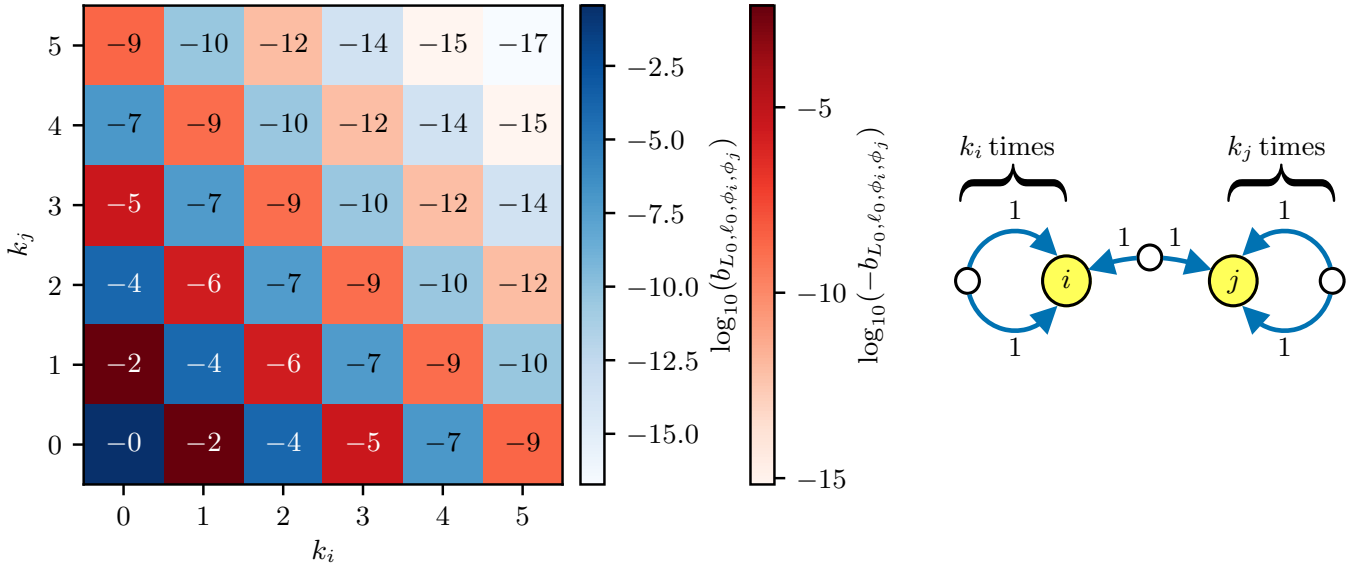


Figure 8. Contributions $b_{L_0, \ell_0, \phi_i, \phi_j}$ of process motifs for correlation with parameters $(L_0, \ell_0, \phi_i, \phi_j)$ for $\theta = 1$, $\varsigma = 1$, and $\epsilon = 0.49$. We show contributions for correlation process motifs that consist of a covariance process motif between node i and node j , a number n_i of variance process motifs at node i , and n_j variance process motifs at node j . All of the process motifs for variance and covariance have parameters $L = 2$ and $\ell = 1$.

lation are process motifs that do not include any process motifs for variance and are thus identical to process motifs for covariance. The process motifs with the largest negative contribution to correlation consist of a process motif for covariance and one process motif for variance at one of the focal nodes.

C. Contributions of structure motifs to covariance and correlation

We now link the process motifs from Section IV B 1 to network structure. For graphlets of up to six edges, we compute the total contribution c and their specific contributions \hat{c} to covariance and correlation in the mOUP at steady state. We first demonstrate that one can explain most of the variation in the total contributions of structure motifs using the total contributions of their subgraphs. We then use the specific contributions of structure motifs to infer mechanisms by which network structure can contribute to covariance and correlation in the mOUP, and we compare the efficiency of these mechanisms.

1. Total contributions of structure motifs to covariance

In Fig. 9, we show the m -edge structure motifs with three largest total contributions to covariance for $m \in \{1, 2, \dots, 6\}$. (Readers can explore the total and specific contributions of further structure motifs using the Jupyter notebook in the Supplementary Materials[84].) There are many aspects of the structure motifs for covari-

ance and their total contributions that one can explore. We focus on two results: (1) one can explain almost the entire variation in c for structure motifs with m edges using the mean total contribution $\langle c \rangle_{m-1}$ of subgraphs with $m-1$ edges; and (2) process motifs are helpful for explaining salient properties of the structure motifs in Fig. 9.

a. Total contributions of subgraphs explain a large portion of the variation in the total contributions of structure motifs. From Fig. 9, we see that, at least up to $m = 6$, the three structure motifs with the largest total contribution c are almost always supergraphs of the $(m-1)$ -edge structure motif with the largest total contribution c . This observation suggests that the total contributions of the subgraphs of a structure motif s have a strong influence on the total contribution of s . To investigate the relationship between the total contributions of structure motifs and the total contributions of their subgraphs, we compute the Pearson correlation coefficient between c of structure motifs with m edges and the mean total contribution of their subgraphs with $m-1$ edges. We show the correlation coefficients in Table I. We observe that one can explain almost all of the variation in c using $\langle c \rangle_{m-1}$. All of the correlation coefficients in Table I are very large, and they increase with the number m of edges and with the mOUP's coupling parameter ϵ .

b. Process motifs explain properties of structure motifs with large total contributions. In thirteen of the sixteen structure motifs in Fig. 9, the focal nodes are connected bidirectionally. Twelve of the structure motifs in Fig. 9 include self-edges. We first explain the high frequency of structure motifs with bidirectionally connected

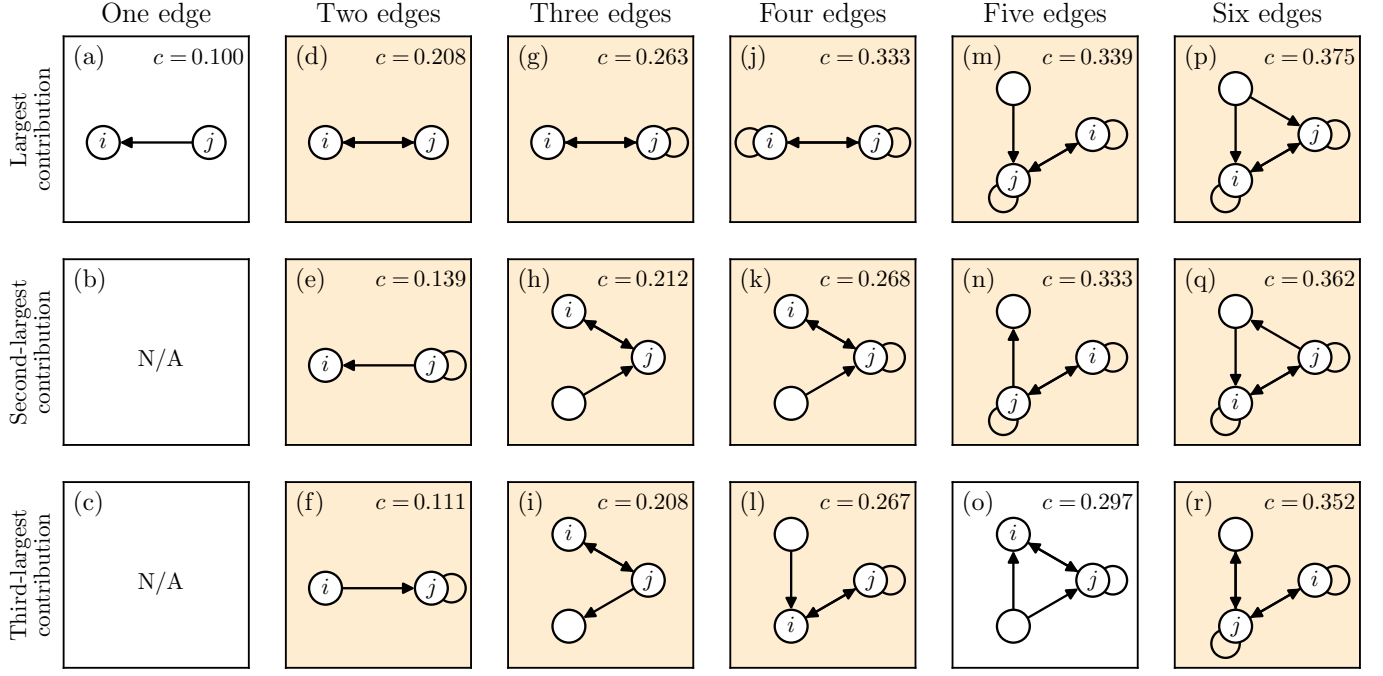


Figure 9. Structure motifs that have the largest total contribution c to covariance between nodes i and j in the mOUP. We round displayed values of c to the third decimal place. Each panel with a peach background shows an m -edge structure motif that is a supergraph of the $(m-1)$ -edge structure motif with the largest total contribution c .

m	Covariance		Correlation	
	$\epsilon = 0.1$	$\epsilon = 0.49$	$\epsilon = 0.1$	$\epsilon = 0.49$
2	0.9985	0.9464	0.9993	0.9806
3	0.9998	0.9932	0.9999	0.9966
4	0.9999	0.9981	> 0.9999	0.9990
5	> 0.9999	0.9993	> 0.9999	0.9996
6	> 0.9999	0.9996	> 0.9999	0.9998

Table I. Pearson correlation coefficients between the total contributions c of m -edge structure motifs to covariance in the mOUP and the mean total contributions $\langle c \rangle_{m-1}$ of subgraphs with $m-1$ edges for different values of the mOUP coupling parameter ϵ . For all of the coefficients that we show, the p -values are less than 10^{-17} .

focal nodes. Whenever a bidirectional edge between focal nodes is part of a structure motif s , the structure motif's total contribution c includes the contributions $b_{L,\ell}$ of all process motifs with odd L . All of these process motifs can occur on s because walks can traverse the bidirectional edge several times. Process motifs with $L=1$ are included in the total contribution of s . They contribute much more to covariance than other process motifs, so s tends to contribute more to covariance than other structure motifs with the same number of edges. For the same reason, a supergraph s'' of s tends to contribute more to covariance than other structure motifs with the same number of edges as s'' .

To explain the high frequency of self-edges in structure

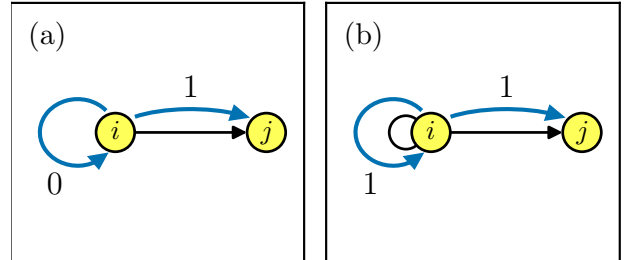


Figure 10. Effect of including a self-edge in a structure motif. In (a), we show a structure motif s with one edge. The curved blue edges with numerical labels indicate the only process motif that can occur on s . In (b), we show s with an additional self-edge at node i . The curved blue edges with numerical labels indicate one of many process motifs that can occur on this structure motif.

motifs with large total contributions to covariance, we consider a structure motif s that does not have a self-edge at either focal node. The inclusion of a self-edge at a focal node in s yields a structure motif s'' that is a supergraph of s . We show a simple example of a structure motif s and a corresponding supergraph s'' in Fig. 10. There are at least twice as many process motifs that can occur on s'' than there are process motifs that can occur on s because for every length- L process motif that can occur on s , there is a length- $(L+1)$ process motif that can occur on s'' but not on s . This example demonstrates that the inclusion of self-edges in a structure motif can

greatly increase its total contribution to covariance.

The high frequencies of self-edges and edges between focal nodes in structure motifs that contribute the most to covariance and correlation suggest that signal transmission via short paths between focal nodes and signal amplification via short cycles are important for mechanisms by which network structure can contribute to covariances of the mOUP.

2. Specific contributions of structure motifs to covariance

In Section III, we proposed to separate the total contribution of a structure motif s into a large part that one can attribute to subgraphs of s and a small part that one cannot attribute to subgraphs of s . This small part \hat{c} is the specific contribution of s . The specific contributions of structure motifs with one edge indicate the contribution to covariance of a single edge. The specific contributions of structure motifs with two edges indicate the contribution to covariance of a pair of edges minus the specific contributions of each of the two edges alone. Whenever the specific contribution of a structure motif is positive, the structure motif indicates a mechanism or a combination of mechanisms by which network structure can enhance covariance.

a. Structure motifs with $\hat{c} > 0$ indicate mechanisms for structure-based enhancement of covariance. In Fig. 11, we show structure motifs with one or two edges and their specific contributions \hat{c} to covariance. Panels (a)–(g) have blue backgrounds and show structure motifs with a positive \hat{c} . These structure motifs indicate mechanisms for enhancing covariance in the mOUP. In panel (h), we include a graphlet that is not a structure motif because it has two components. We include it because it is helpful for discussing the mechanisms by which network structure can contribute to covariance in the mOUP. The positive specific contributions for structure motifs in panels (a) and (e) indicate that signal transmission via short paths from one focal node to the other can increase covariance. The positive specific contributions for structure motifs in panels (b) and (d) indicate that signal amplification via a length-1 cycle can increase covariance when combined with a path for signal transmission between focal nodes. The specific contribution of the graphlet in panel (h) is 0, which indicates that, without any connection between focal nodes, signal amplification at a focal node does not increase covariance. In panel (f), the bidirectional edge between focal nodes enables signal transmission from either focal node to the other. It also creates a 2-cycle at each focal node. The positive specific contributions for structure motifs in panels (c) and (g) indicate that a signal transmission from a non-focal node can contribute to covariance. Comparing panels (c) and (g) to panel (k), we see that a positive \hat{c} requires that there are paths from the non-focal node to both focal nodes. The 0 contributions of the structure motifs in panels (i), (j), and (l) indicate that paths from

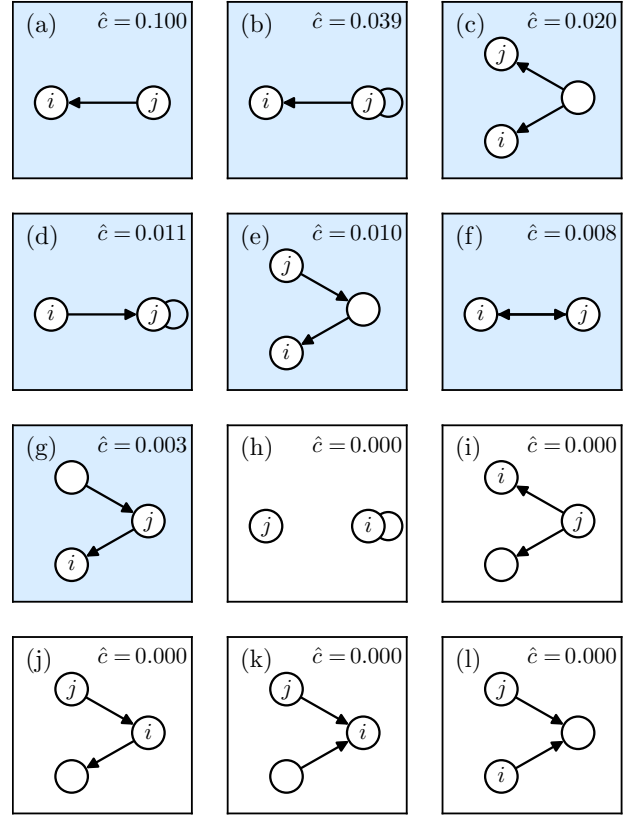


Figure 11. Structure motifs with one or two edges and their specific contributions \hat{c} to covariance. We round displayed values of c to the fourth decimal place. Panels (a)–(g) have blue backgrounds and show structure motifs with a positive \hat{c} .

focal nodes to other nodes are not relevant for covariance between focal nodes.

From these observations, we conclude that two mechanisms for increasing covariance in the mOUP are (1) signal transmission via paths from one focal node to another and (2) signal transmission from non-focal nodes that are connected to both focal nodes via paths from the non-focal node to each focal node. Other mechanisms for increasing covariance in the mOUP are combinations of signal transmission via paths between focal nodes and signal transmission from non-focal nodes. Such mechanisms can also be combinations of either or both mechanisms with signal amplification via short cycles at focal nodes or other nodes.

b. Specific contributions indicate the efficiency of mechanisms. Thus far, we have used specific contributions to distinguish structure motifs with $\hat{c} > 0$ and thus contribute to covariance from structure motifs with $\hat{c} = 0$ that thus do not contribute to covariance. We can use the value of specific contributions to define a measure of efficiency of a mechanism that is associated with a structure motif. For a structure motif with m edges and specific

contribution \hat{c} , we define the efficiency

$$\eta := \hat{c}/m.$$

From Fig. 11, we see that specific contributions and thus η tend to decrease with the number of edges in a structure motif. The mechanisms with large efficiency tend to be associated with small structure motifs. The structure motif with the largest \hat{c} for covariance (see Fig. 11(a)) indicates direct signal transmission (i.e., signal transmission via a length-1 path) as a mechanism for increasing covariance. The associated efficiency is $\eta \approx 0.1$. All other mechanisms have much smaller efficiencies than direct signal transmission. For example, signal transmission via a length-2 path (see Fig. 11(e)) has $\eta \approx 0.005$, and ones through longer paths are even smaller.

When the focal nodes are connected by a single directed path, one can think of the focal node with positive out-degree as the “sender” node and the node with positive in-degree as the “receiver” node. The second-most efficient mechanism is a combination of direct signal transmission and signal amplification via a length-1 cycle at the sender node (see Fig. 11(b)). This mechanism has an efficiency of $\eta \approx 0.02$. The efficiency of direct signal transmission with signal amplification via a length-1 cycle at the receiver node (see Fig. 11(d)) has an efficiency of $\eta \approx 0.005$, which is almost four times smaller than the previous mechanisms. Transmission of signals from a third node to both focal nodes via length-1 paths (see Fig. 11(c)) has an efficiency of $\eta \approx 0.01$.

c. Matching motifs give a heuristic way to explain specific contributions. For the mechanisms that are associated with 1-edge and 2-edge structure motifs, one can explain the ranking of specific contributions using matching process motifs. The total contribution of structure motif s is the sum of contributions of process motifs p that can occur on s . If p contributes to the specific contribution \hat{c} of s , the process motif p uses each edge in s at least once because otherwise p would contribute to the specific contribution of a proper subgraph of s . Contributions of process motifs tend to decrease with the length of process motifs. Therefore, the largest contributions of process motifs to \hat{c} of s come from matching process motifs of s . One can use the sum

$$\gamma := \sum_{p \in P_s} b(p)$$

of contributions of matching process motifs as a heuristic for estimating \hat{c} of s . We show the Pearson correlation coefficients for \hat{c} and γ for different structure-motif lengths in Table II. For comparison, we also show a second heuristic $\gamma' = \max_{p \in P_s} b(p)$ that only uses the contribution of the process motifs on s that contributes the most to covariance. We observe a large positive correlation between \hat{c} and γ for all considered structure-motif lengths. The heuristic γ is correlated most strongly with \hat{c} when both m and ϵ are small. The heuristic γ' also has a large pos-

itive correlation with \hat{c} for $m = 2$. However, as we consider s with progressively more edges, the Pearson correlation coefficient between s and γ' decreases much faster than the Pearson correlation coefficient between s and γ . This difference between the two heuristics demonstrates that, for structure motifs with more than two edges, it is important to consider all matching process motifs with just one matching process motif.

m	Covariance		Correlation	
	$\epsilon = 0.1$	$\epsilon = 0.49$	$\epsilon = 0.1$	$\epsilon = 0.49$
2	0.998	0.966	0.962	0.900
3	0.996	0.903	0.958	0.855
4	0.994	0.814	0.913	0.723
5	0.996	0.879	0.854	0.718
6	0.993	0.820	0.811	0.606

Table II. Pearson correlation coefficients for the heuristics γ and γ' with specific contribution \hat{c} of m -edge structure motifs to covariances of the mOUP with a coupling parameter of ϵ . For all of these Pearson correlation coefficients, the p-values are less than 0.00017.

3. Specific contributions of structure motifs to correlation

We demonstrated in Section IV C that specific contributions of structure motifs indicate covariance-enhancing mechanisms more clearly than total contributions. In this section, we focus on specific contributions of structure motifs to correlations in the mOUP. In Fig. 12, we show the m -edge structure motifs with the three largest specific contributions to correlation for $m \in \{1, 2, \dots, 6\}$. (Readers can explore the total and specific contributions of further structure motifs using the Jupyter notebook in the Supplementary Materials[84].)

a. Network structure can increase or decrease correlations. In Fig. 13, we show structure motifs with one or two edges and their specific contributions \hat{c} to correlation in the mOUP.

Negative specific contributions to correlation in the mOUP indicate that there are mechanisms by which network structure can decrease the correlation between a pair of nodes in the mOUP. The structure motifs with negative \hat{c} for correlation include structure motifs that have 0 specific contribution to covariance. An example is the structure motif in Fig. 13(j). Its specific contribution to covariance is $\hat{c} = 0$, from which we concluded in Section IV C 2 that signal transmission from a non-focal node to only one focal node does not increase covariance in the mOUP. The same structure motif has a negative specific contribution to correlation in the mOUP. Therefore, we conclude that signal transmission from a non-focal node to a single focal node can decrease correlation in the mOUP.

The structure motifs with negative \hat{c} for correlation

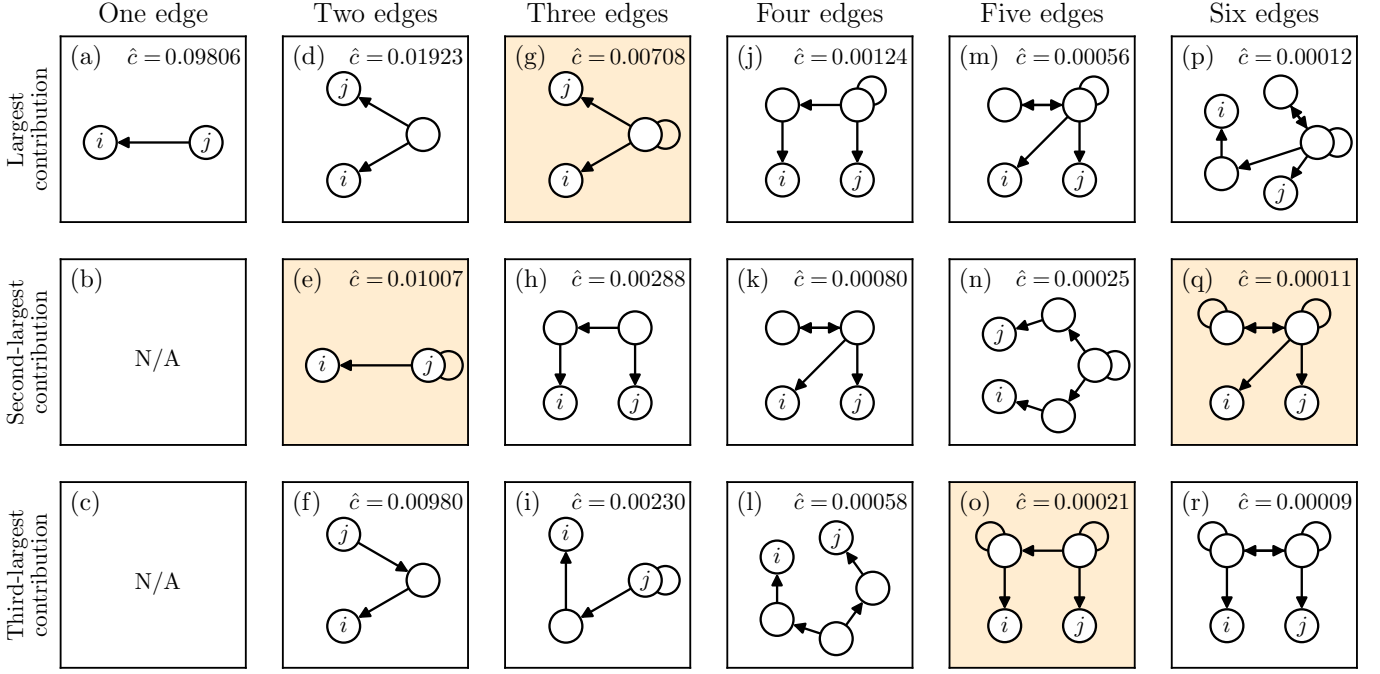


Figure 12. Structure motifs that have the largest specific contribution \hat{c} to the correlation between nodes i and j in the mOUP. We round the displayed values of \hat{c} to the fifth decimal place. Each panel with a peach background shows an m -edge structure motif that is a supergraph of the $(m-1)$ -edge structure motif with the largest specific contribution \hat{c} .

also include structure motifs that have a positive \hat{c} for covariance. An example is the structure motif in Fig. 13(l). In Section IV C 2, we concluded that direct signal transmission with signal amplification at the receiver node is a mechanism by which network structure can increase covariance in the mOUP. From the structure motif's negative specific contribution to correlation, we conclude that, by the same mechanism, network structure can decrease correlation in the mOUP.

b. The ranking of mechanisms by efficiency is different for covariance and correlation. Comparing the specific contributions to covariance and correlation for a given structure motif, we see that the contributions are almost identical for some structure motifs. For example, the structure motif in Fig. 13(a) has $\hat{c} \approx 0.1000$ for covariance and $\hat{c} \approx 0.098$ for correlation. Another example is the structure motif in Fig. 13(b). It has $\hat{c} \approx 0.02$ for covariance and $\hat{c} \approx 0.019$ for correlation. For other structure motifs, the specific contributions to correlation are much smaller than their specific contributions to covariance. For example, the structure motif in Fig. 13(c) has $\hat{c} \approx 0.39$ for covariance and $\hat{c} \approx 0.01$ for correlation.

This difference between the specific contributions to covariance and correlation is related to the process motifs for variance in focal nodes. Structure motifs on which few long process motifs for focal-node variance node can occur tend to have very similar specific contributions to covariance and correlation. Examples of such structure motifs are the ones in Fig. 13(a) and (b). For other structure motifs, the specific contributions to covariance

and correlation are very different. The structure motif in Fig. 13(c) is an example of this observation. Due to these differences, ranking structure motifs by specific contribution to covariance and ranking structure motifs by their specific contribution to correlation leads to different rankings. Consequently, the rankings based on efficiency of the associated mechanisms are also different.

c. Increasing the in-degree of a receiver node reduces correlations in locally tree-like networks. The structure motifs in Figs. 13(e), (g), (h), and (j) include a directed edge between focal nodes and an in-edge or out-edge at the sender node or the receiver node. We use these structure motifs and their specific contributions to correlation to study the effect on increasing the in-degree or out-degree of focal nodes on correlations in a locally tree-like network [85]. For locally tree-like networks, one assumes that neighbors of a node are not neighbors of each other. We also assume that we can neglect the structure motifs with more than two edges because such structure motifs tend to have very small values of \hat{c} (see Fig. 12). Under these assumptions, we note the following:

1. an increase of the in-degree of a sender node leads to an increase of the count of the structure motif in Fig. 13(e) but no others,
2. an increase of the out-degree of a sender node leads to an increase of the count of the structure motif in Fig. 13(g) but no others,
3. an increase of the in-degree of a receiver node leads to an increase of the count of the structure motifs

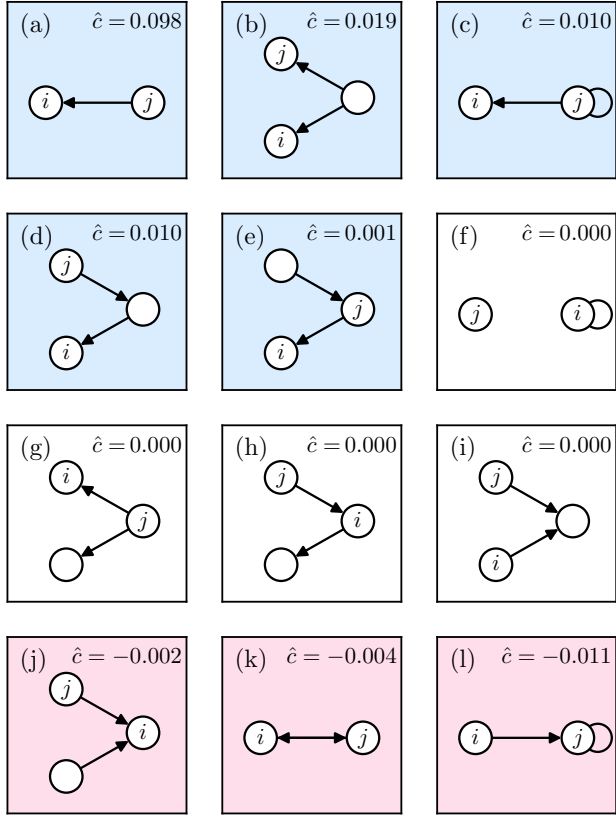


Figure 13. Structure motifs with one or two edges and their specific contributions \hat{c} to correlation. We round displayed values of c to the fourth decimal place. Panels (a)–(e) show structure motifs with a positive \hat{c} and have blue backgrounds. Panels (j)–(l) show structure motifs with a negative \hat{c} and have pink backgrounds.

in Fig. 13(h) but no others, and

4. an increase of the out-degree of a receiver node leads to an increase of the count of the structure motifs in Fig. 13(j) but no others.

One can infer the effect of increasing in-degree or out-degree of the sender node or the receiver node from the specific contributions of these structure motifs. Increasing the out-degree of the sender node (see Fig. 13(g)) or the receiver node (see Fig. 13(f)) does not affect the correlation between the sender and the receiver. Increasing the in-degree of the the sender node (see Fig. 13(e)) has a small positive effect on correlation. Increasing the in-degree of the receiver node (see Fig. 13(j)) has a negative effect on correlation.

When two focal nodes are connected bidirectionally, one cannot distinguish between a sender node and a receiver node. Increasing the in-degree of either focal node increases the counts of the structure motif in Fig. 13(e) and the structure motif in Fig. 13(j) by 1 each. The net effect of increasing the in-degree of a focal node is given by the sum of the specific contributions of the structure motifs in Fig. 13(e) and (j) and is negative. Increasing

the in-degree of a node in a locally tree-like network thus reduces the correlation between this node and nodes with which it is connected bidirectionally.

V. CONCLUSIONS AND DISCUSSION

Discovering connections between dynamics on networks and network structure is an ongoing endeavor of researchers in many disciplines. Many researchers have considered it helpful to decompose networks into structural building blocks, which are typically called "motifs". In the present paper, we demonstrated that combining such a decomposition of a network's structure into structure motifs with a decomposition of processes on a network into process motifs can yield both mechanistic and quantitative insights into connections between dynamics on networks and network structure. To construct a framework for the combined decomposition of processes on networks and network structure, we introduced walk graphs as "building blocks" of processes and defined contributions of process motifs and total contributions and specific contributions of structure motifs to observables of dynamical systems on networks.

A. Mechanisms for enhancing covariance and correlation in the Ornstein–Uhlenbeck process

To demonstrate our framework, we performed a combined decomposition into process and structure motifs for the multivariate Ornstein–Uhlenbeck process (mOUP) on a network. We identified the process motifs that contribute to variances, covariances, and correlations in the mOUP at steady state. We then used the contributions of the identified process motifs to variance, covariance, and correlation to explain the total contributions and specific contributions of structure motifs to covariance and correlation. The specific contributions of structure motifs indicate several mechanisms by which network structure can enhance the covariance or the correlation between two focal nodes in the mOUP at steady state. We found that edges in structure motifs can positively contribute to covariance and correlation by

1. enhancing signal transmission between two focal nodes,
2. signal amplification at either focal node, and/or
3. signal transmission from other nodes to both focal nodes.

Structure motifs contribute positively to covariance or correlation by enhancing signal transmission between focal nodes; signal transmission from non-focal nodes; or a combination of signal transmission between focal nodes, signal transmission from non-focal nodes, and signal amplification at focal nodes or non-focal nodes. The ranking

of structure motifs and associated mechanisms by specific contributions is different for covariance and correlation, and it depends on the coupling parameter ϵ of the mOUP.

Some of our results on process motifs and structure motifs for covariance and correlation for the mOUP may match a reader’s intuition for covariance and correlation. For example, the popular phrase “correlation does not imply causation” is consistent with our results that (1) process motifs for covariance or correlation between two nodes i and j do not necessarily include a walk from i to j or from j to i and (2) structure motifs for covariance or correlation do not necessarily include a path or trail from i to j or from j to i . Our results confirm known results about the mechanisms by which network structure can affect covariances and correlations between variables, and they also offer new quantitative insights into the efficiency of these mechanisms and the relationship between efficiency and the parameters of the mOUP.

B. Applicability to other dynamical systems

In the present paper, we studied covariance and correlation in a simple stochastic dynamical system at steady state. We chose this example for illustrative purposes and to demonstrate that our approach can confirm and extend intuition about the network mechanisms that contribute to system function. It is possible to apply our framework to other system functions, other linear dynamical systems, and away from a steady state. (For dynamical systems that are away from a steady state, process-motif decompositions of system functions can depend on motif counts and initial conditions.)

We considered structure motifs in directed networks with self-edges. For some systems in biology, chemistry, sociology, and other areas, it can be more appropriate to consider undirected networks or networks without self-edges than to consider directed networks with self-edges. One can apply our framework to these networks by focusing motif comparison to structure motifs in undirected networks or networks without self-edges. Because of the flexibility of our approach, we anticipate that the study of process motifs can yield insights into many open problems in the study of dynamical systems on networks.

C. When does the distinction between process motifs and structure motifs matter?

The distinction between process motifs and structure motifs matters for many but not all dynamical systems. Our core motivation for distinguishing between process motifs and structure motifs is that a walk on a network and a path in a network are two fundamentally different concepts. A walk can use an edge in a network several times, whereas a path or trail can include each edge only once. When one defines a process on a network such that it can use each node only once, the distinction between

walks and paths becomes unnecessary because every path corresponds to a single walk.

Examples of relevant dynamical processes include susceptible–infected (SI) models and susceptible–infected–recovered (SIR) models for the spread of an infectious disease [66, 86], because infected and recovered individuals in these models cannot become infected a second time; consequently, a disease can spread along each edge at most once. One can construct other models that allow recurring infections (i.e., an individual can become infected multiple times). Examples of such models are susceptible–infected–susceptible (SIS) models and susceptible–infected–recovered–susceptible (SIRS) models. For such models, it is important to distinguish between process motifs and structure motifs. One can circumvent the need to make a distinction by introducing restrictive model assumptions that are popular in the modeling of infectious diseases [66]. For example, one can assume that

1. a network is a directed acyclic graph (DAG) or
2. a network is directed and locally tree-like and that the infection rates are low.

On a DAG, there are no process motifs that use an edge in a network more than once. Under assumption (1), the distinction between process motifs and structure motifs does not matter. In networks that are both directed and locally tree-like, there are no process motifs of length $L \leq 3$ that use an edge in a network more than once. A low infection rate ensures that contributions of long process motifs are very small. Under assumption (2), the distinction between process motifs and structure motifs then has only a small effect on the specific contributions of structure motifs. We anticipate that distinguishing between process motifs and structure motifs can aid researchers in the study of diseases on networks with models in which recurring infections are possible.

When a network is a DAG, walks on it cannot use an edge more than once. The distinction between process motifs and structure motifs is thus not relevant for any dynamical system on a DAG. There are numerous applications of dynamical systems on DAGs in machine learning and neuroscience [87, 88]. They include feed-forward artificial neural networks and models of natural neural networks in the visual cortex of several species [89, 90]. Many researchers in machine learning and neuroscience have highlighted the fundamental differences in the dynamics of non-recurrent neural networks (i.e., neural networks that are DAGs) and recurrent networks (i.e., networks that are not DAGs) [87, 91]. We anticipate that our framework for decomposing processes on networks into process motifs can help explain some of these differences between non-recurrent and recurrent neural networks.

Dynamical systems on temporal networks are another example for which one can sometimes ignore the distinction between process motifs and structure motifs. One

can define many temporal networks such that each edge is active only at a specified point in time or during a specified time interval [92]. When each edge in a temporal network is active only at very few times points or only for time intervals that are short compared to the temporal scales of processes on a network, few or no walks on the temporal network use an edge more than once. For dynamical systems on temporal networks for which the edge dynamics are comparably as fast as or faster than the dynamics on the network, it is possible that each structure motif has only a few associated process motifs. (See [86] for a discussion of the relative temporal scales of dynamics on networks and dynamics of networks.) The development of new notions of structure motifs in temporal networks is an active field of research, and researchers have made several proposals for notions of structure motifs in temporal networks [93–96]. The distinction between process motifs and structure motifs may be helpful for assessing these proposals and the development of further notions of motifs on temporal networks.

D. “Unbiased” mechanistic insights from process motifs and structure motifs

In this paper, we presented an approach for identifying graphlets that are relevant to a function of a system. Our approach offers several advantages over traditional approaches, in which researchers use overrepresentation of graphlets to conclude the relevance of graphlets to a system function. Those approaches depend strongly on the choice of a random-graph null model [17–19], and they do not identify mechanisms by which overrepresented graphlets affect a system function. Studies of dynamical systems on graphlets in isolation require researchers to choose a graphlet and a candidate mechanism *a priori*. The reliance on these choices makes such studies prone to bias towards graphlets or mechanisms that a researcher has chosen to study. For example, many studies have reported the relevance of feedback loops and feed-forward loops for various system functions [2]. However, it is unclear if these two graphlets are generally more important for system functions than other graphlets or if researchers have associated them more frequently than other graphlets with system function because they have studied them more often.

Our approach identifies all structure motifs with a positive (or negative) contribution to a given function of a dynamical system. The approach is unbiased in the sense that its results do not depend on an *a priori* choice of a graphlet or a mechanism. Our results for covariance and correlation in the mOUP demonstrate that there can be many structure motifs that affect a system function. Had we considered only a single graphlet in our study, it is likely that we would have concluded that that graphlet affects covariance and correlation in the mOUP and would then have inferred that that graphlet is impor-

tant for these system functions. Our systematic study of all graphlets with up to six edges enabled us to rank structure motifs based on their contribution strengths and made it possible to distinguish between structure motifs that strongly affect covariance and correlation in the mOUP and structure motifs that have smaller (or even negligible) contributions to these system functions.

We also demonstrated how one can conduct a combined decomposition of dynamics on a network and network structure into process motifs and structure motifs. One can use such a decomposition to identify structure motifs that contribute the most to a given system function and to explain how these structure motifs contribute to the system function. We demonstrated that it can be useful to consider dynamics on a network (instead of just a network’s structure) as a composite object that one can decompose into many small parts. Our proposed framework thereby provides an opportunity to develop insights into mechanisms by which dynamics and network structure affect system functions.

ACKNOWLEDGEMENTS

We thank Alex Arenas, Lionel Barnett, Heather Zinn Brooks, Bing Brunton, Michelle Feng, Kameron Decker Harris, Renaud Lambiotte, Neave O’Cleary, Gesine Reinert, and Jonny Wray for helpful discussions and comments. A.C.S. was supported by the Engineering and Physical Sciences Research Council under grant number EP/L016044/1, the Clarendon Fund, and e-Therapeutics plc. M.A.P. acknowledges support from the National Science Foundation (grant number 1922952) through the Algorithms for Threat Detection (ATD) program.

Appendix A: Derivation of a non-recursive formula for the specific contributions of structure motifs

Consider a structure motif s with m edges with specific contribution \hat{c}_s . Successive recursions of Eq. (4) lead to an expression that depends only on the total contributions c_t of subgraphs t of s . Subgraphs with the same number $m' < m$ of edges contribute to \hat{c}_s in the same way. One can thus write

$$\begin{aligned} \hat{c}_s = & \alpha_1 \langle c \rangle_1 + \alpha_2 \langle c \rangle_2 + \alpha_3 \langle c \rangle_3 + \dots \\ & + \alpha_{m-1} \langle c \rangle_{m-1} + \alpha_m \langle c \rangle_m, \end{aligned} \quad (A1)$$

where $\alpha_{m'}$, where $m' \in \{1, \dots, m\}$, are integer coefficients and $\langle c \rangle_{m'}$ is the mean total contribution of subgraphs with m' edges. The structure motif s has exactly one subgraph (specifically, the graph itself) with m edges, so $\langle c \rangle_m = c_s$. From Eq. (4), one can see that $\alpha_m = 1$ in the “0-th” recursion of Eq. (4). Further recursions of Eq. (4) do not change α_m because subgraphs with m edges are not proper subgraphs of s and thus do not appear in the sum over proper subgraphs $t \subset s$ in

Eq. (4). The first recursion of Eq. (4) yields

$$\hat{c}_s = c_s - \sum_{t_1 \subset s} \left(c_{t_1} - \sum_{t_2 \subset t_1} \hat{c}_{t_2} \right). \quad (\text{A2})$$

From Eq. (A2), one can see that α_{m-1} is equal to the negative of the number of subgraphs of s with $m-1$ edges in the first recursion of Eq. (4). Further recursions of Eq. (4) do not change α_{m-1} , because subgraphs with $m-1$ edges cannot be proper subgraphs of proper subgraphs t_1 of s and thus do not appear in the sum over proper subgraphs $t_2 \subset t_1$. It thus follows that

$$\alpha_{m-1} = - \binom{m}{m-1}.$$

Subgraphs with $m-2$ edges are proper subgraphs of s . We thus obtain $\alpha_{m-2} = - \binom{m}{m-2}$ in the first recursion of Eq. (4). Because subgraphs with $m-2$ edges are also proper subgraphs of proper subgraphs t_1 of s , the second recursion of Eq. (4) leads to an additional term $\binom{m}{m-1} \binom{m-1}{m-2}$ in α_{m-2} . Further recursions of Eq. (4) do not change α_{m-2} . It thus follows that

$$\alpha_{m-2} = - \binom{m}{m-2} + \binom{m}{m-1} \binom{m-1}{m-2}$$

Similar considerations lead to

$$\begin{aligned} \alpha_{m-3} &= - \binom{m}{m-3} + \binom{m}{m-1} \binom{m-1}{m-3} \\ &\quad + \binom{m}{m-2} \binom{m-2}{m-3} \\ &\quad + \binom{m}{m-1} \binom{m-1}{m-2} \binom{m-2}{m-3}. \end{aligned}$$

We see that each coefficient $\alpha_{m'}$ includes one or several products of binomial coefficients. Each of these products has the form

$$\binom{m}{m_1} \binom{m_1}{m_2} \cdots \binom{m_{k-2}}{m_{k-1}} \binom{m_{k-1}}{m'}$$

for some $k \leq m-m'$. Such a product of binomial coefficients corresponds to the number of ways that one can partition the edge set of s into k subsets with sizes

$$\begin{aligned} m - m_1, m_1 - m_2, \dots, \\ m_{k-2} - m_{k-1}, m_{k-1} - m', m'. \end{aligned}$$

The coefficient $\alpha_{m'}$ includes one such term for each integer composition of m that includes m' . It follows that

$$\alpha_{m'} = \sum_{\mathbf{q} \in \mathcal{Q}(m-m')} (-1)^{|\mathbf{q}|} \binom{m}{m'} \mathbf{q}!, \quad (\text{A3})$$

where $\mathcal{Q}(m-m')$ is the set of integer compositions $\mathbf{q} = (q_1, q_2, \dots, q_k)$ of $m-m'$ and $\mathbf{q}! := (q_1, q_2, \dots, q_k)!$ is the multinomial coefficient for the sequence (q_1, q_2, \dots, q_k) of k integers. We use $|\mathbf{q}| := k$ to denote the number of integers in an integer composition \mathbf{q} . Substituting the coefficients $\alpha_{m'}$ into Eq. (A1) with Eq. (A3) yields Eq. (5).

Appendix B: Derivation of the covariance matrix

At time $t+dt$, the state vector of the mOUP with adjacency matrix \mathbf{A} , coupling parameter ϵ , noise amplitude ς^2 , and reversion rate θ is

$$\mathbf{x}_{t+dt} = \mathbf{K} \mathbf{x}_t + \varsigma dW_t, \quad (\text{B1})$$

where $\mathbf{K} = \mathbf{I} + \theta(\epsilon \mathbf{A} - \mathbf{I})dt$. At steady-state, the mOUP has the covariance matrix

$$\Sigma = \langle \mathbf{x}_t \mathbf{x}_t^T \rangle = \langle \mathbf{x}_{t+dt} \mathbf{x}_{t+dt}^T \rangle, \quad (\text{B2})$$

where $\langle \cdot \rangle$ denotes an ensemble average. Using Eq. (B1), we substitute \mathbf{x}_{t+dt} into Eq. (B2) to obtain

$$\begin{aligned} \Sigma &= \langle (\mathbf{K} \mathbf{x}_t + \varsigma dW_t)(\mathbf{K} \mathbf{x}_t + \varsigma dW_t)^T \rangle \\ &= \langle \mathbf{K} \mathbf{x}_t \mathbf{x}_t^T \mathbf{K}^T + \varsigma^2 \mathbf{I} dt \rangle, \end{aligned} \quad (\text{B3})$$

where the second equality follows from the fact that dW_t is a mean-0, unit-variance stochastic process that is independent of \mathbf{x}_t . Evaluating the ensemble average in Eq. (B3) yields

$$\begin{aligned} \Sigma &= \mathbf{K} \Sigma \mathbf{K}^T + \varsigma^2 \mathbf{I} dt \\ &= [\mathbf{I} + \theta(\epsilon \mathbf{A} - \mathbf{I})(dt)^2] \Sigma [\mathbf{I} + \theta(\epsilon \mathbf{A} - \mathbf{I})(dt)^2]^T \\ &\quad + \varsigma^2 \mathbf{I} (dt)^2 \\ &= \Sigma + \theta \left[(\epsilon \mathbf{A} - \mathbf{I}) \Sigma + \Sigma (\epsilon \mathbf{A} - \mathbf{I})^T + \frac{\varsigma^2}{\theta} \mathbf{I} \right] dt \\ &\quad + O((dt)^2). \end{aligned}$$

To first order in dt , we thus have

$$0 = (\epsilon \mathbf{A} - \mathbf{I}) \Sigma + \Sigma (\epsilon \mathbf{A} - \mathbf{I})^T + \frac{\varsigma^2}{\theta} \mathbf{I}. \quad (\text{B4})$$

Equation (B4) is a Lyapunov equation [97, 98]. For the mOUP with signal decay, the solution of Eq. (B4) is [97]

$$\Sigma = \frac{\varsigma^2}{\theta} \int_0^\infty e^{(\epsilon \mathbf{A} - \mathbf{I})t} e^{(\epsilon \mathbf{A}^T - \mathbf{I})t} dt = \frac{\varsigma^2}{\theta} \Sigma_0, \quad (\text{B5})$$

where

$$\Sigma_0 := \int_0^\infty e^{(\epsilon \mathbf{A} - \mathbf{I})t} e^{(\epsilon \mathbf{A}^T - \mathbf{I})t} dt$$

is the covariance matrix of the mOUP when $\varsigma = \theta = 1$. For $\varsigma = \theta = 1$, Barnett et al. [23, 41] derived the covariance matrix as a sum of products of \mathbf{A} and \mathbf{A}^T [99]:

$$\Sigma_0 = \sum_{L=0}^{\infty} 2^{-(L+1)} \sum_{\ell=0}^L \binom{L}{\ell} (\epsilon \mathbf{A})^\ell (\epsilon \mathbf{A}^T)^{L-\ell}. \quad (\text{B6})$$

Therefore,

$$\Sigma = \frac{\varsigma^2}{\theta} \sum_{L=0}^{\infty} 2^{-(L+1)} \sum_{\ell=0}^L \binom{L}{\ell} (\epsilon \mathbf{A})^\ell (\epsilon \mathbf{A}^T)^{L-\ell}. \quad (\text{B7})$$

Appendix C: Conditions for short-range signal decay

The sums in Eq. (13) converge if the matrix $\Sigma_0 = \frac{\theta}{\varsigma^2} \Sigma$ has eigenvalues $\nu_{i=1,\dots,n} \in (0, 1)$ [100, p. 38]. The covariance matrix Σ_0 is a symmetric positive semidefinite matrix. A sufficient condition for short-range signal decay thus only needs to constrain the largest eigenvalue of Σ_0 .

First, we show that a sufficient condition for short-range signal decay is

$$\|\epsilon \mathbf{A}\|_2 < \frac{1}{2}. \quad (\text{C1})$$

Applying the Hilbert–Schmidt norm to both sides of Eq. (B6) yields

$$\begin{aligned} \|\Sigma_0\|_2 &= \left\| \sum_{L=0}^{\infty} 2^{-(L+1)} \sum_{\ell=0}^L \binom{L}{\ell} (\epsilon \mathbf{A}^T)^\ell (\epsilon \mathbf{A})^{L-\ell} \right\|_2 \\ &\leq \sum_{L=0}^{\infty} 2^{-(L+1)} \sum_{\ell=0}^L \binom{L}{\ell} \|\epsilon \mathbf{A}\|_2^L \\ &= \frac{1}{2} \sum_{L=0}^{\infty} \|\epsilon \mathbf{A}\|_2^L, \end{aligned}$$

where we used the identity $\|\mathbf{A}^T\|_2 = \|\mathbf{A}\|_2$ and subadditivity and submultiplicativity of the Hilbert–Schmidt norm. When $\|\epsilon \mathbf{A}\|_2 < 1/2$, it follows that $\|\Sigma_0\|_2 < 1$, so $\nu_{i=1,\dots,n} \in (0, 1)$ for the positive-semidefinite matrix Σ_0 . It follows that the sums in Eq. (13) converge.

For many applications in network analysis, the spectral radius $\rho(\cdot)$ (which is equal to the largest absolute eigenvalue of a matrix) is a commonly used matrix norm

[101, 102]. We now show that one can relax the condition in Eq. (C1) for short-range signal decay to

$$\rho(\mathbf{A}) < \frac{1}{2} \quad (\text{C2})$$

if \mathbf{A} is the adjacency matrix of a strongly connected graph with non-negative edge weights.

The adjacency matrix of a strongly connected graph is irreducible [103]. For an irreducible matrix with non-negative entries, the Perron–Frobenius theorem guarantees the existence of a simple, real, positive eigenvalue $\lambda_{\max} = \rho(\mathbf{A})$ [103]. The transpose of \mathbf{A} is also an adjacency matrix of a strongly connected graph with non-negative edge weights, so \mathbf{A}^T also has a simple positive real leading eigenvalue λ_{\max} . Ortega [104, p. 24] proved the existence of a submultiplicative matrix norm $\|\mathbf{M}\|$, such that $\rho(\mathbf{M}) = \|\mathbf{M}\|$ for all complex square matrices \mathbf{M} with simple max-modulus eigenvalues [105]. The matrices \mathbf{A} and \mathbf{A}^T are matrices with a single simple max-modulus eigenvalue. We thus write

$$\begin{aligned} \rho(\Sigma_0) &\leq \|\Sigma_0\| \\ &\leq \left\| \sum_{L=0}^{\infty} 2^{-(L+1)} \sum_{\ell=0}^L \binom{L}{\ell} (\epsilon \mathbf{A}^T)^\ell (\epsilon \mathbf{A})^{L-\ell} \right\| \end{aligned}$$

and use the subadditivity and submultiplicativity of $\|\cdot\|$ to obtain

$$\rho(\Sigma) \leq \frac{1}{2} \sum_{L=0}^{\infty} \|\epsilon \mathbf{A}\|^L = \frac{1}{2} \sum_{L=0}^{\infty} (\rho(\epsilon \mathbf{A}))^L. \quad (\text{C3})$$

When $\rho(\epsilon \mathbf{A}) < 1/2$, it follows from Eq. (C3) that $\rho(\Sigma_0) < 1$. It follows that $\nu_{i=1,\dots,n} \in (0, 1)$, so the sums in Eq. (13) converge.

[1] S. S. Shen-Orr, R. Milo, S. Mangan, and U. Alon, Network motifs in the transcriptional regulation network of *Escherichia coli*, *Nature Genetics* **31**, 64 (2002).

[2] U. Alon, Network motifs: Theory and experimental approaches, *Nature Reviews Genetics* **8**, 450 (2007).

[3] L. Stone, D. Simberloff, and Y. Artzy-Randrup, Network motifs and their origins, *PLoS Computational Biology* **15**, e1006749 (2019).

[4] J. M. Rip, K. S. McCann, D. H. Lynn, and S. Fawcett, An experimental test of a fundamental food web motif, *Proceedings of the Royal Society of London B: Biological Sciences* **277**, 1743 (2010).

[5] K. Ristl, S. J. Plitzko, and B. Drossel, Complex response of a food-web module to symmetric and asymmetric migration between several patches, *Journal of Theoretical Biology* **354**, 54 (2014).

[6] T. Ohnishi, H. Takayasu, and M. Takayasu, Network motifs in an inter-firm network, *Journal of Economic Interaction and Coordination* **5**, 171 (2010).

[7] F. W. Takes, W. A. Kosters, B. Witte, and E. M. Heemskerk, Multiplex network motifs as building blocks of corporate networks, *Applied Network Science* **3**, 39 (2018).

[8] K. Juszczyk, K. Musiał, P. Kazienko, and B. Gabrys, Temporal changes in local topology of an email-based social network, *Computing and Informatics* **28**, 763 (2012).

[9] X. Hong-Lin, Y. Han-Bing, G. Cui-Fang, and Z. Ping, Social network analysis based on network motifs, *Journal of Applied Mathematics* **2014** (2014).

[10] R. Milo, S. Shen-Orr, S. Itzkovitz, N. Kashtan, D. Chklovskii, and U. Alon, Network motifs: Simple building blocks of complex networks, *Science* **298**, 824 (2002).

[11] G. C. Conant and A. Wagner, Convergent evolution of gene circuits, *Nature Genetics* **34**, 264 (2003).

[12] O. Sporns and R. Kötter, Motifs in brain networks, *PLoS Biology* **2**, e369 (2004).

[13] P. J. Ingram, M. P. Stumpf, and J. Stark, Network motifs: Structure does not determine function, *BMC Genomics* **7**, 108 (2006).

[14] M. Golubitsky, L. Shiau, C. Postlethwaite, and

Y. Zhang, The feed-forward chain as a filter-amplifier motif, in *Coherent Behavior in Neuronal Networks* (Springer-Verlag, Heidelberg, Germany, 2009) pp. 95–120.

[15] F. Antoneli, M. Golubitsky, and I. Stewart, Homeostasis in a feed forward loop gene regulatory motif, *Journal of Theoretical Biology* **445**, 103 (2018).

[16] A. Shilnikov, R. Gordon, and I. Belykh, Polyrhythmic synchronization in bursting networking motifs, *Chaos: An Interdisciplinary Journal of Nonlinear Science* **18**, 037120 (2008).

[17] Y. Artzy-Randrup, S. J. Fleishman, N. Ben-Tal, and L. Stone, Comment on “Network motifs: simple building blocks of complex networks” and “Superfamilies of evolved and designed networks”, *Science* **305**, 1107 (2004).

[18] S. Robin, S. Schbath, and V. Vandewalle, Statistical tests to compare motif count exceptionalities, *BMC Bioinformatics* **8**, 84 (2007).

[19] W. E. Schlauch and K. A. Zweig, Influence of the null-model on motif detection, in *2015 IEEE/ACM International Conference on Advances in Social Networks Analysis and Mining (ASONAM)* (IEEE, 2015) pp. 514–519.

[20] In other studies, the term “structural motif” often has been used to refer to structure motifs, but it sometimes has been used to refer to process motifs. We give an overview of the use of motifs in the study of networks in Section II E. We use the terms “structure motif” and “process motif” to avoid confusion with conflicting definitions of “structural motif” in previous work by other scholars. We use the composite nouns to stress that we consider structure motifs and process motifs to be two fundamentally different concepts.

[21] Note that we distinguish a “system function” (which may, for example, be a biological function in a system) from a “mathematical function” like Y .

[22] O. O. Aalen and H. K. Gjessing, Survival models based on the Ornstein–Uhlenbeck process, *Lifetime Data Analysis* **10**, 407 (2004).

[23] L. Barnett, C. L. Buckley, and S. Bullock, Neural complexity and structural connectivity, *Physical Review E* **79**, 051914 (2009).

[24] Z. Liang, K. C. Yuen, and J. Guo, Optimal proportional reinsurance and investment in a stock market with Ornstein–Uhlenbeck process, *Insurance: Mathematics and Economics* **49**, 207 (2011).

[25] R. V. Rohlfs, P. Harrigan, and R. Nielsen, Modeling gene expression evolution with an extended Ornstein–Uhlenbeck process accounting for within-species variation, *Molecular Biology and Evolution* **31**, 201 (2013).

[26] D. Grytskyy, T. Tetzlaff, M. Diesmann, and M. Helias, A unified view on weakly correlated recurrent networks, *Frontiers in Computational Neuroscience* **7**, 131 (2013).

[27] Y. Hu, J. Trousdale, K. Josić, and E. Shea-Brown, Local paths to global coherence: Cutting networks down to size, *Physical Review E* **89**, 032802 (2014).

[28] M. D. Fox and M. Greicius, Clinical applications of resting state functional connectivity, *Frontiers in Systems Neuroscience* **4** (2010).

[29] S. L. Carter, C. M. Brechbühler, M. Griffin, and A. T. Bond, Gene co-expression network topology provides a framework for molecular characterization of cellular state, *Bioinformatics* **20**, 2242 (2004).

[30] J.-P. Onnela, K. Kaski, and J. Kertész, Clustering and information in correlation based financial networks, *The European Physical Journal B* **38**, 353 (2004).

[31] H. Reichenbach, *The Direction of Time* (University of California Press, Berkeley and Los Angeles, CA, USA, 1956).

[32] B. Bollobás, *Modern Graph Theory*, Vol. 184 (Springer, Berlin, Germany, 2013).

[33] R. J. Trudeau, *Introduction to Graph Theory* (Dover Publications, New York, NY, USA, 2013).

[34] Other researchers have defined a path to be a combination of nodes and edges without repetitions [106]. Using this definition, a path is a special case of a walk. For our work, it is crucial to distinguish paths and walks as two fundamentally different concepts, where the former is related to processes on networks and the latter is related to network structure.

[35] D. Spielman, Spectral graph theory, in *Combinatorial Scientific Computing* (CRC Press, Boca Raton, Florida, USA, 2012).

[36] N. Alon, C. Avin, M. Koucký, G. Kozma, Z. Lotker, and M. R. Tuttle, Many random walks are faster than one, *Combinatorics, Probability and Computing* **20**, 481 (2011).

[37] C. Godsil and K. Guo, Quantum walks on regular graphs and eigenvalues, *The Electronic Journal of Combinatorics* **18**, P165 (2011).

[38] G. H. Nguyen, J. B. Lee, R. A. Rossi, N. K. Ahmed, E. Koh, and S. Kim, Continuous-time dynamic network embeddings, in *Companion Proceedings of the The Web Conference 2018* (2018) pp. 969–976.

[39] Ö. N. Yaveroğlu, N. Malod-Dognin, D. Davis, Z. Levnajic, V. Janjic, R. Karapandza, A. Stojmirovic, and N. Pržulj, Revealing the hidden language of complex networks, *Scientific Reports* **4**, 4547 (2014).

[40] G. Wu, M. Harrigan, and P. Cunningham, Classifying wikipedia articles using network motif counts and ratios, in *Proceedings of the Eighth Annual International Symposium on Wikis and Open Collaboration*, 12 (2012) pp. 1–10.

[41] L. Barnett, C. L. Buckley, and S. Bullock, Neural complexity: A graph theoretic interpretation, *Physical Review E* **83**, 041906 (2011).

[42] J. T. Lizier, F. M. Atay, and J. Jost, Information storage, loop motifs, and clustered structure in complex networks, *Physical Review E* **86**, 026110 (2012).

[43] L. Novelli, F. M. Atay, J. Jost, and J. T. Lizier, Deriving pairwise transfer entropy from network structure and motifs, *Proceedings of the Royal Society A* **476**, 20190779 (2020).

[44] G. Ciriello and C. Guerra, A review on models and algorithms for motif discovery in protein–protein interaction networks, *Briefings in Functional Genomics and Proteomics* **7**, 147 (2008).

[45] A. Masoudi-Nejad, F. Schreiber, and Z. R. M. Kashani, Building blocks of biological networks: A review on major network motif discovery algorithms, *Iet Systems Biology* **6**, 164 (2012).

[46] F. Battiston, V. Nicosia, M. Chavez, and V. Latora, Multilayer motif analysis of brain networks, *Chaos: An Interdisciplinary Journal of Nonlinear Science* **27**, 047404 (2017).

[47] J. B. Dechery and J. N. MacLean, Functional triplet motifs underlie accurate predictions of single-trial responses in populations of tuned and untuned V1 neu-

rons, PLoS Computational Biology **14**, e1006153 (2018).

[48] G. C. Garcia, A. Lesne, M.-T. Hütt, and C. C. Hilgetag, Building blocks of self-sustained activity in a simple deterministic model of excitable neural networks, Frontiers in Computational Neuroscience **6**, 50 (2012).

[49] V. P. Zhigulin, Dynamical motifs: Building blocks of complex dynamics in sparsely connected random networks, Physical Review Letters **92**, 238701 (2004).

[50] P. M. Gleiss, P. F. Stadler, A. Wagner, and D. A. Fell, Relevant cycles in chemical reaction networks, Advances in Complex Systems **4**, 207 (2001).

[51] A. Vazquez, R. Dobrin, D. Sergi, J.-P. Eckmann, Z. N. Oltvai, and A.-L. Barabási, The topological relationship between the large-scale attributes and local interaction patterns of complex networks, Proceedings of the National Academy of Sciences of the United States of America **101**, 17940 (2004).

[52] K. Shen, G. Bezgin, R. M. Hutchison, J. S. Gati, R. S. Menon, S. Everling, and A. R. McIntosh, Information processing architecture of functionally defined clusters in the macaque cortex, Journal of Neuroscience **32**, 17465 (2012).

[53] Y. Iturria-Medina, R. C. Sotero, E. J. Canales-Rodríguez, Y. Alemán-Gómez, and L. Melie-García, Studying the human brain anatomical network via diffusion-weighted MRI and Graph Theory, Neuroimage **40**, 1064 (2008).

[54] G. Bianconi, Number of cycles in off-equilibrium scale-free networks and in the internet at the autonomous system level, The European Physical Journal B **38**, 223 (2004).

[55] S. Manrubia and J. Poyatos, Motif selection in a model of evolving replicators: The role of surfaces and limited transport in network topology, Europhysics Letters **64**, 557 (2003).

[56] A. Ma'ayan, G. A. Cecchi, J. Wagner, A. R. Rao, R. Iyengar, and G. Stolovitzky, Ordered cyclic motifs contribute to dynamic stability in biological and engineered networks, Proceedings of the National Academy of Sciences of the United States of America **105**, 19235 (2008).

[57] O. Sporns, G. Tononi, and G. M. Edelman, Theoretical neuroanatomy: Relating anatomical and functional connectivity in graphs and cortical connection matrices, Cerebral Cortex **10**, 127 (2000).

[58] O. Sporns, G. Tononi, and G. M. Edelman, Connectivity and complexity: The relationship between neuroanatomy and brain dynamics, Neural Networks **13**, 909 (2000).

[59] E. Estrada and J. A. Rodriguez-Velazquez, Subgraph centrality in complex networks, Physical Review E **71**, 056103 (2005).

[60] J. Trousdale, Y. Hu, E. Shea-Brown, and K. Josić, Impact of network structure and cellular response on spike time correlations, PLoS Computational Biology **8**, e1002408 (2012).

[61] S. Jovanović and S. Rotter, Interplay between graph topology and correlations of third order in spiking neuronal networks, PLoS Computational Biology **12** (2016).

[62] G. Tononi, O. Sporns, and G. M. Edelman, A measure for brain complexity: Relating functional segregation and integration in the nervous system, Proceedings of the National Academy of Sciences of the United States of America **91**, 5033 (1994).

[63] C. Börgers, *An Introduction to Modeling Neuronal Dynamics* (Springer, Cham, Switzerland, 2017).

[64] S. Lehmann and Y.-Y. Ahn, *Complex Spreading Phenomena in Social Systems* (Springer, Cham, Switzerland, 2018).

[65] R. Pastor-Satorras, C. Castellano, P. Van Mieghem, and A. Vespignani, Epidemic processes in complex networks, Reviews of Modern Physics **87**, 925 (2015).

[66] I. Z. Kiss, J. C. Miller, and P. L. Simon, *Mathematics of Epidemics on Networks* (Springer, Cham, Switzerland, 2017).

[67] G. Demirel, F. Vazquez, G. Böhme, and T. Gross, Moment-closure approximations for discrete adaptive networks, Physica D: Nonlinear Phenomena **267**, 68 (2014).

[68] T. House, G. Davies, L. Danon, and M. J. Keeling, A motif-based approach to network epidemics, Bulletin of Mathematical Biology **71**, 1693 (2009).

[69] S. Chandra, E. Ott, and M. Girvan, Critical network cascades with re-excitable nodes: Why treelike approximations usually work, when they break down, and how to correct them, Physical Review E **101**, 062304 (2020).

[70] S.-W. Oh and M. A. Porter, Complex contagions with timers, Chaos: An Interdisciplinary Journal of Nonlinear Science **28**, 033101 (2018).

[71] D. T. Haydon, M. Chase-Topping, D. J. Shaw, L. Matthews, J. K. Friar, J. Wilesmith, and M. E. J. Woolhouse, The construction and analysis of epidemic trees with reference to the 2001 uk foot-and-mouth outbreak, Proceedings of the Royal Society of London. Series B: Biological Sciences **270**, 121 (2003).

[72] J. S. Juul and S. H. Strogatz, Descendant distributions for the impact of mutant contagion on networks, Physical Review Research **2**, 033005 (2020).

[73] M. E. J. Newman, Spread of epidemic disease on networks, Physical Review E **66**, 016128 (2002).

[74] F. Radicchi and C. Castellano, Leveraging percolation theory to single out influential spreaders in networks, Physical Review E **93**, 062314 (2016).

[75] D. B. Larremore, M. Y. Carpenter, E. Ott, and J. G. Restrepo, Statistical properties of avalanches in networks, Physical Review E **85**, 066131 (2012).

[76] G. Bianconi, Epidemic spreading and bond percolation on multilayer networks, Journal of Statistical Mechanics: Theory and Experiment **2017**, 034001 (2017).

[77] An “integer composition” of a non-negative number m is a sequence (q_1, q_2, \dots, q_k) of positive integers, where $\sum_{k'=1}^k q_{k'} = m$ [107].

[78] G. E. Uhlenbeck and L. S. Ornstein, On the theory of the Brownian motion, Physical Review **36**, 823 (1930).

[79] M.-T. Tsai, J.-D. Saphores, and A. Regan, Valuation of freight transportation contracts under uncertainty, Transportation Research Part E: Logistics and Transportation Review **47**, 920 (2011).

[80] T. Sanderson, G. Hertzler, T. Capon, and P. Hayman, A real options analysis of australian wheat production under climate change, Australian Journal of Agricultural and Resource Economics **60**, 79 (2016).

[81] C. P. Ogbogbo, Modeling crude oil spot price as an Ornstein–Uhlenbeck process, International Journal of Mathematical Analysis and Optimization: Theory and Applications **2018**, 261 (2018).

[82] J. Rice, *Mathematical Statistics and Data Analysis*, 3rd ed. (Thomson Higher Education, Belmont, CA, USA, 2006).

[83] B. Barzel and O. Biham, Quantifying the connectivity of a network: The network correlation function method, *Physical Review E* **80**, 046104 (2009).

[84] The Jupyter notebook is available as a web application under <https://gitlab.com/aliceschwarze/motifs-for-processes>.

[85] S. Melnik, A. Hackett, M. A. Porter, P. J. Mucha, and J. P. Gleeson, The unreasonable effectiveness of tree-based theory for networks with clustering, *Physical Review E* **83**, 036112 (2011).

[86] M. A. Porter and J. P. Gleeson, Dynamical Systems on Networks, *Frontiers in Applied Dynamical Systems: Reviews and Tutorials* **4** (2016).

[87] P. Tino, L. Benuskova, and A. Sperduti, Artificial neural network models, in *Springer Handbook of Computational Intelligence* (Springer, Cham, Switzerland, 2015) pp. 455–471.

[88] T. Shinozaki and S. Watanabe, Structure discovery of deep neural network based on evolutionary algorithms, in *2015 IEEE International Conference on Acoustics, Speech and Signal Processing (ICASSP)* (2015) pp. 4979–4983.

[89] R. VanRullen and C. Koch, Visual selective behavior can be triggered by a feed-forward process, *Journal of Cognitive Neuroscience* **15**, 209 (2003).

[90] B. M. Kampa, J. J. Letzkus, and G. J. Stuart, Cortical feed-forward networks for binding different streams of sensory information, *Nature Neuroscience* **9**, 1472 (2006).

[91] G. Manjunath and H. Jaeger, Echo state property linked to an input: Exploring a fundamental characteristic of recurrent neural networks, *Neural Computation* **25**, 671 (2013).

[92] P. Holme and J. Saramäki, *Temporal Network Theory* (Springer, Cham, Switzerland, 2019).

[93] A. Paranjape, A. R. Benson, and J. Leskovec, Motifs in temporal networks, in *Proceedings of the Tenth ACM International Conference on Web Search and Data Mining* (2017) pp. 601–610.

[94] K. Tu, J. Li, D. Towsley, D. Braines, and L. D. Turner, Network classification in temporal networks using motifs, arXiv:1807.03733 (2018).

[95] P. Liu, V. Guarasi, and A. E. Sarıyüce, Temporal network motifs: Models, limitations, evaluation, arXiv:2005.11817 (2020).

[96] J. M. Roldan, V. K. George, G. A. Silva, *et al.*, Construction of edge-ordered multidirected graphlets for comparing dynamics of spatial temporal neural networks, arXiv:2006.15971 (2020).

[97] F. W. Fairman, *Linear Control Theory: The State Space Approach* (John Wiley & Sons, New York City, NY, USA, 1998).

[98] C.-T. Chen, *Linear System Theory and Design*, 4th ed. (Oxford University Press, Inc., Oxford, United Kingdom, 2013).

[99] In [23, 41], the order of \mathbf{A} and \mathbf{A}^T is reversed, because the authors used row vectors instead of column vectors to describe the state \mathbf{x}_t .

[100] B. Hall, *Lie Groups, Lie Algebras, and Representations: An Elementary Introduction*, Vol. 222 (Springer-Verlag, Cham, Switzerland, 2015).

[101] A. Jamakovic, R. Kooij, P. Van Mieghem, and E. R. van Dam, Robustness of networks against viruses: The role of the spectral radius, in *IEEE 2006 Symposium on Communications and Vehicular Technology* (2006) pp. 35–38.

[102] D. Stevanovic, *Spectral Radius of Graphs* (Academic Press, London, UK, 2014).

[103] M. Boyle, Notes on the Perron–Frobenius theory of non-negative matrices (2015).

[104] J. M. Ortega, *Numerical Analysis: A Second Course* (SIAM, Philadelphia, PA, USA, 1990).

[105] A max-modulus eigenvalue μ of a matrix \mathbf{M} is an eigenvalue that satisfies $\mu = \rho(\mathbf{M})$.

[106] M. E. J. Newman, *Networks* (Oxford University Press, Oxford, United Kingdom, 2018).

[107] S. Eger, Restricted weighted integer compositions and extended binomial coefficients, *Journal of Integer Sequences* **16**, 3 (2013).